Program Definition Status Report:
Short-Baseline Neutrino Oscillation Program on the Fermilab Booster Neutrino Beam

The Short Baseline Neutrino Program Task Force
Peter Wilson
FNAL, SBN Program Coordinator

Alberto Guglielmi
INFN, Sezione di Padua

Marzio Nessi
CERN

David Schmitz
Univ. of Chicago

Geralyn Zeller
FNAL

July 21, 2014

ABSTRACT

We describe the status of developing a comprehensive Fermilab Short-Baseline Neutrino (SBN) oscillation program consisting of three LAr TPC detectors located at near, medium, and far locations on the Fermilab Booster Neutrino Beam.

CONTENTS

I. INTRODUCTION

At the January 2014 meeting of the Fermilab PAC, presentations were made by two collaborations to significantly enhance the physics capabilities of the Booster Neutrino Beam (BNB) with additional LAr TPC detectors. Both proposals were targeted at providing definitive measurements of the LSND and MiniBooNE anomalies. The ICARUS collaboration proposed [1] a two detector experiment incorporating the existing T600 LAr TPC located 700 m from the BNB as a far detector and a new T150 LAr TPC located 150±50 m from the target as a near detector. The primary physics goal of the ICARUS proposal was the search for light sterile neutrinos. The LAr1-ND collaboration proposed [2] to install a new LAr TPC based on LBNE-type technology 100 m from the BNB target in an existing enclosure that was constructed for the SciBooNE experiment. The proposed LAr1-ND detector, in concert with the MicroBooNE experiment, would address the MiniBooNE neutrino mode anomaly and enable improved searches for oscillations through the ν_e appearance and ν_μ disappearance channels.

Following the recommendation of the PAC, the MicroBooNE, LAr1-ND, and ICARUS collaborations were asked by the Fermilab Director to propose a combined Short-Baseline Neutrino (SBN) program to address the short-baseline anomalies and search for sterile neutrinos. The Director appointed a SBN Program Coordinator to assist the collaborations in establishing this program. The first major step in establishing this program was a three day workshop at Fermilab in April 2014 that drew 25 participants. Members of all three collaborations were joined by representatives from the LBNE project, Fermilab engineering, and the NESSiE collaboration. The primary results of the workshop were: establishment of a common basis for evaluating experimental sensitivity, deciding on an initial baseline configuration for the program, and establishing connections between the collaborations for further development of the program.

A SBN Task Force was created shortly after the April workshop to steer the activities required to establish a conceptual design for the program. The task-force consists of five members, one representing each of the three collaborations (LAr1-ND, MicroBooNE, ICARUS), one representing CERN, and the Fermilab SBN Program Coordinator. The CERN participation in SBN is part of an initiative to establish a broad-based collaboration between CERN and Fermilab on future neutrino experiments. The Task Force immediately established four working groups to address key issues identified at the workshop:

1. Cosmic backgrounds,

2. Neutrino flux and systematics,

3. Detector building configuration and siting,

4. Cryostat and cryogenic system design and integration.

The first two working groups, each co-lead by members of LAr1-ND and ICARUS, are aimed at determining the optimal configuration of the experiments (e.g. baseline of near detector)

based on analyses of the impact on the physics sensitivity. The latter two working groups, each co-lead by a member of ICARUS and Fermilab staff, are aimed at refining experimental configurations for the purpose of establishing schedules and cost. This report will summarize the current state of the work of these four groups and the plans for their future activities. Although some conclusions have been reached, the working groups are expected to continue at least until a Conceptual Design Report has been completed. The scope of the working groups activities or the number of working groups is likely to evolve as the work of defining the program progresses toward that design.

Section II of this document provides a brief description of the physics motivation for the SBN program. In addition to the physics motivation, the near detector is intended as a detector R&D initiative that will provide a near term test-bed for LAr TPC technology with benefits to the long-baseline neutrino program. Potential benefits include expanded experience in construction of membrane cryostats, development of standardized cryogenic system modules, wire plane assembly techniques, and testing of next generation cold electronics.

Section III describes a configuration optimization of detector positioning driven by physics sensitivity of the program. The first study is on impact of uncertainties in the understanding of the flux at the far and near detectors as a function of the near detector location. Studies of the flux systematics indicate that there is no significant difference in sensitivity between locating the near detector at 110m, 150m or 200m from the BNB target. Cross-checks to fully validate this analysis are in progress. Since there is a cost advantage to using the SciBooNE enclosure to house the cryogenic system for the experiment, the reference design has the near detector located at 110m. Although other systematics have not yet been analyzed with the same level of detail, an initial enumeration of the relevant systematics has been made and is included in this document.

The impact of cosmogenic backgrounds is also discussed in Section III. Although a full analysis of the cosmic backgrounds has not yet been conducted, several independent simulations have been performed with similar results. Estimates of the background of cosmogenic photons faking an electron have been made. Counting only those background electrons in the beam spill time ($1.6\mu s$) rather than the drift time ($\sim$1ms), the background is estimated to be at a scale similar to electrons from the intrinsic ν_e content of the beam at the location of the proposed T600 far detector (600m) with shielding. All of the simulations come to the same conclusion to within about a factor of two. Investigation of mitigation strategies such as light detection to provide the necessary timing and topological selections are just starting. Since this full analysis has not yet been performed, the baseline building designs have the capability of including cosmic ray shielding.

Section IV describes the current reference configuration of the program. Based on the results of the work on flux systematics, the reference location for the near detector is 100m from the BNB target in a new enclosure adjacent to the SciBooNE enclosure and the far detector located at 600m. Both detectors will be located on the beam axis with the capability for installing shielding to reduce cosmogenic backgrounds.

Section V describes the schedule, funding, and organization of the program. A draft set

of high level milestones is proposed that culminate in a three detector configuration ready for beam data-taking in the spring of 2018. A conceptual design along with cost and schedule are foreseen to be ready for review in the fall of 2014. Funding for the program is expected from a combination of DOE, NSF, and international in-kind contributions. Since the program is not expected to undergo the DOE critical decision process, a structure is proposed that would be administered as a series of Fermilab Director's reviews.

II.   MOTIVATION: SHORT-BASELINE ANOMALIES AND THE SEARCH FOR LIGHT STERILE NEUTRINOS

In this section, we briefly review the various experimental results that hint at the possibility of new physics occurring in the neutrino sector. We include this description for completeness, but refer the reader to more thorough descriptions of these results and their interpretation, including [3, 4] and the references therein.

In recent years, experimental "anomalies" ranging in statistical significance (2.8–3.8σ) have been reported from a variety of experiments studying neutrinos over baselines less than 1 km. Two distinct classes of anomalies pointing at additional physics beyond the Standard Model in the neutrino sector have been reported, namely a) the apparent reduction in the ν_e low energy neutrinos from nuclear reactors [12] (the "reactor anomaly") and from Mega-Curie radioactive neutrino sources in the Gallium experiments [13] originally designed to detect solar neutrinos (the "Gallium anomaly"), and b) evidence for an electron-like excess in interactions coming from neutrinos from particle accelerators [5, 8] (the "LSND and MiniBooNE anomalies"). None of these results can be described by oscillations between the three Standard Model neutrinos and, therefore, could be hinting at important new physics.

A.   LSND $\bar{\nu}_\mu \to \bar{\nu}_e$

The Liquid Scintillator Neutrino Detector experiment (LSND) was conducted at Los Alamos National Laboratory from 1993 through 1998. LSND used a decay-at-rest (DAR) pion beam to produce a beam of $\bar{\nu}_\mu$ between 20-53 MeV about 30 m from a liquid scintillator-based detector. $\bar{\nu}_e$ were detected through inverse beta decay (IBD) on carbon, $\bar{\nu}_e p \to e^+ n$. The signature of IBD events is a prompt positron followed by a 2.2 MeV γ produced when the neutron captures on free protons in the scintillator. After 5 years of data taking, $89.7\pm22.4\pm6.0$ $\bar{\nu}_e$ candidate events were observed above backgrounds, corresponding to 3.8σ evidence for $\bar{\nu}_\mu \to \bar{\nu}_e$ oscillations [5] occurring at a Δm^2 in the 1 eV^2 region. This signal, therefore, cannot be accommodated with the three Standard Model neutrinos, and like the other short-baseline hints for oscillations at $L/E_\nu \sim 1$ m/MeV, implies new physics.
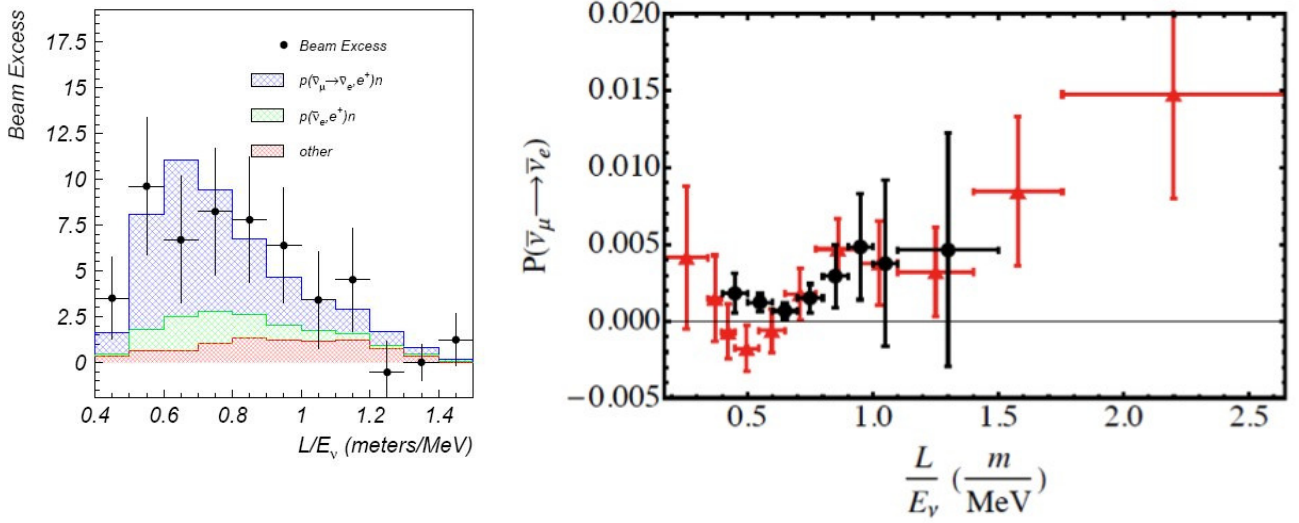
FIG. 1: *Left: Excess of electron neutrino candidate events observed by the LSND experiment [5]. Right: Oscillation probability as a function of L/E_ν if the excess candidate events are assumed due to $\bar{\nu}_\mu \rightarrow \bar{\nu}_e$ transitions using MiniBooNE (red) and LSND (black) data.*

B.   MiniBooNE $\nu_\mu \rightarrow \nu_e$ and $\bar{\nu}_\mu \rightarrow \bar{\nu}_e$

The MiniBooNE collaboration has recently completed an analysis of their full ten year data set including both neutrino and anti-neutrino running [6–9]. The MiniBooNE detector sits 540 m downstream of the Booster Neutrino Beam target at Fermilab. Predominately muon flavor neutrinos are produced in pion decay-in-flight, yielding a broad beam with a peak energy around 700 MeV. Muon and electron neutrinos are identified in charged-current interactions by the characteristic signatures of Cherenkov rings for muons and electrons.

MiniBooNE observes a 3.4σ signal excess of ν_e candidates in neutrino mode (162.0 ± 47.8 electromagnetic events). These events, along with backgrounds, are shown in Figure 2. The excess events can be electrons or single photons since these are indistinguishable in MiniBooNE's Cherenkov imaging detector. MicroBooNE will address this question at the same baseline as MiniBooNE by applying the LAr TPC technology to separately identify electrons and photons.

MiniBooNE also observes an excess of 78.4 ± 28.5 electron anti-neutrino candidates (2.8σ) at both low and somewhat higher energies than in neutrinos as shown in Figure 2. Figure 1 compares the L/E_ν dependence of these events to the excess observed at LSND. It is this signal in anti-neutrino mode that the full multi-detector SBN program could address.

C.   Reactor neutrino anomaly

A re-evaluation of the $\bar{\nu}_e$ flux produced by nuclear power reactors [10, 11] has prompted a re-analysis of short baseline reactor $\bar{\nu}_e$ disappearance measurements from the last several
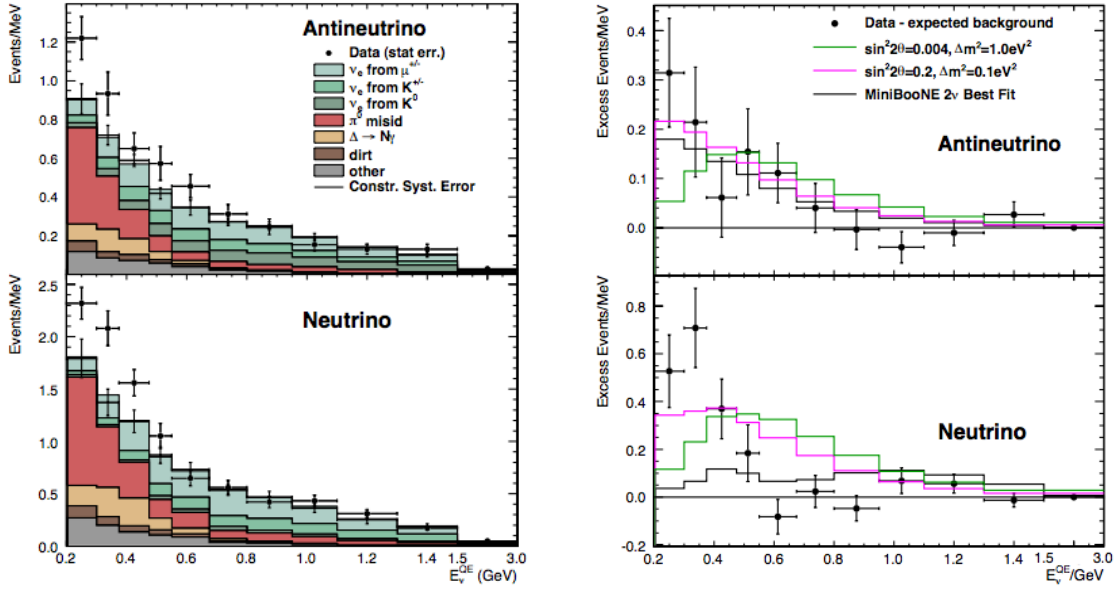
FIG. 2: *Left: $\bar{\nu}_e$ (top) and ν_e (bottom) candidate events and predicted backgrounds showing the observed excesses in the MiniBooNE data. Right: background subtracted event rates in the MiniBooNE anti-neutrino (top) and neutrino (bottom) data [8]. E_ν^{QE} refers to the reconstructed neutrino event energy, where a quasi-elastic interaction is assumed in the reconstruction.*

decades [12]. The new reference spectra takes advantage of a re-evaluation of inverse beta decay cross sections impacting the neutron lifetime and accounts for long-lived radioisotopes accumulating in reactors. Figure 3 shows this predicted flux compared to reactor measurements as a function of the baseline of each experiment. With this new prediction, the observed rates of interactions in detectors between 10 and 100 meters from the reactors are, on average, 6–7% lower than that expected in the absence of oscillations. Depending on the analysis of the systematic uncertainties on the absolute reactor flux predictions, this amounts to a discrepancy of 1.4–3.0σ. This result could be explained through $\bar{\nu}_e$ disappearance due to oscillations at Δm^2 ~1 eV^2, which could be consistent with the MiniBooNE and LSND appearance anomalies.

D. GALLEX and SAGE calibration data

Both the GALLEX and SAGE solar neutrino experiments used test sources to calibrate their detectors. In total, they ran four test runs: two in GALLEX and one in SAGE with a ^{51}Cr source which emits a 750 keV ν_e and one in SAGE with a ^{37}Ar source, an 810 keV ν_e emitter. The test data reveal a deficit of electron neutrinos relative to the predicted rate as shown in Figure 4. The best fit ratio of data to prediction is 0.86 ± 0.05 [13]. This deficit of very low energy electron neutrinos over very short baselines could also be explained through ν_e disappearance due to oscillations at $\Delta m^2 \geq 1$ eV^2.
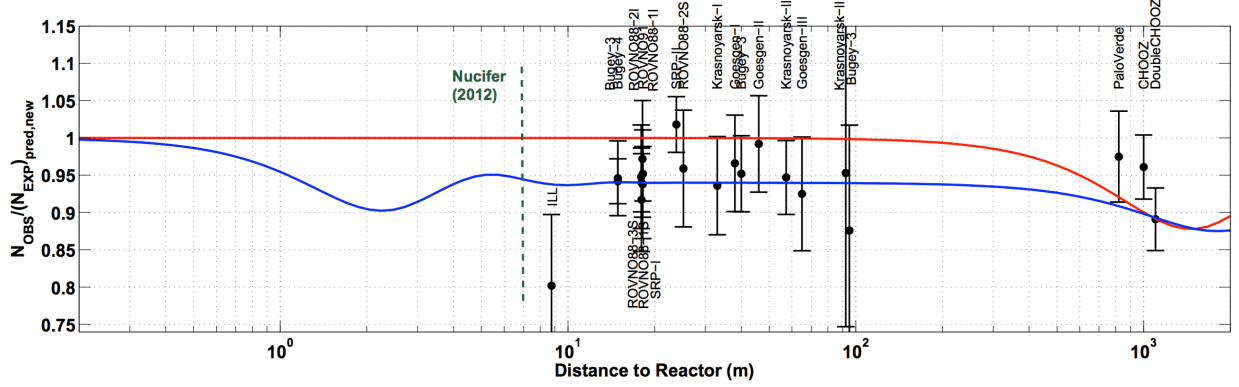
FIG. 3: *Ratio of the observed to predicted reactor $\bar{\nu}_e$ rate for 19 different reactor neutrino experiments at baselines less than 100 m. The mean average ratio including correlations is 0.927 ± 0.023, indicating a 7.3% deficit at these short-baselines. The curves show fits to the data assuming standard three neutrino oscillations (red) and assuming 3+1 neutrino oscillations including one additional sterile neutrino state (blue) [12].*
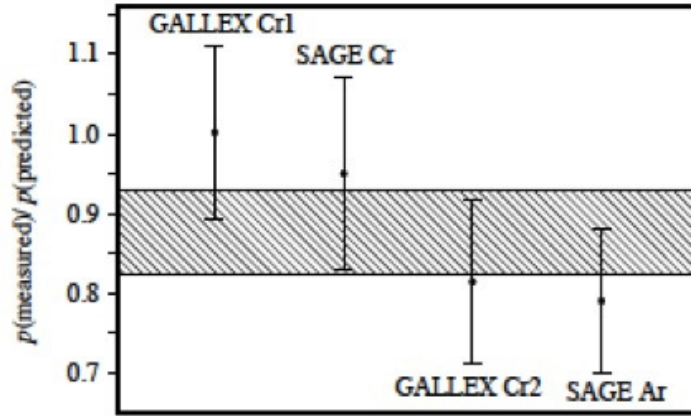
FIG. 4: *The measured/predicted event ratio for the GALLEX and SAGE source calibration data. The average, shown by the shaded band, is 0.86 ± 0.05 [13].*

E. Interpretation

Table I summarizes the results discussed above and lists their individual significance. While each of these measurements taken separately lack the significance to claim a discovery, together these signals could be hinting at important new physics. The most common interpretation is evidence for the possible existence of one or more additional, mostly "sterile" neutrino states

Experiment	Type	Channel	Significance
LSND	DAR	$\bar{\nu}_\mu \to \bar{\nu}_e$ CC	3.8σ
MiniBooNE	SBL accelerator	$\nu_\mu \to \nu_e$ CC	3.4σ
MiniBooNE	SBL accelerator	$\bar{\nu}_\mu \to \bar{\nu}_e$ CC	2.8σ
GALLEX/SAGE	Source - e capture	ν_e disappearance	2.8σ
Reactors	Beta-decay	$\bar{\nu}_e$ disappearance	3.0σ

TABLE I: *Summary of the experimental hints suggesting the possibility of high-Δm^2 neutrino oscillations.*

with masses at or below the few eV range. In these models, the mass states ν_1, ν_2 and ν_3 are those responsible for the well established oscillations observed at $\Delta m_{21}^2 = 7.5 \times 10^{-5}$ eV^2 and $\Delta m_{31}^2 = 2.4 \times 10^{-3}$ eV^2 and are taken to be dominated by active flavors (ν_e, ν_μ, ν_τ) with only small contributions from sterile flavors. Additional higher mass neutrino states, ν_4, ν_5, ... are taken as mostly sterile with small active flavor content. The experimental results described above can be interpreted as indications of oscillations due to mass-squared splitting in the $\Delta m_{41}^2 \approx [0.1 - 10]$ eV^2 range.

Constraints on sterile neutrino mixing from ν_μ and neutral-current disappearance data are also available. An explanation of all the available hints in terms of oscillations suffers from significant tension between appearance and disappearance data [4], particularly due to the absence of ν_μ disappearance in the $\Delta m^2 \sim 1$ eV^2 region.

In the simplest extension to the 3-neutrino model, a single mostly sterile mass eigenstate, ν_4, can be added (Figure 5). In such a 3+1 model, ν_e appearance and ν_μ disappearance probabilities are described by:

$$P_{\nu_\alpha \to \nu_\beta}^{3+1} = \delta_{\alpha\beta} - 4 \left| U_{\alpha 4} \right|^2 \left(\delta_{\alpha\beta} - \left| U_{\beta 4} \right|^2 \right) \sin^2 \left(\frac{\Delta m_{41}^2 L}{4 E_\nu} \right) \tag{1}$$

where U_{ij} are elements of the now 4×4 mixing matrix, $\Delta m_{41}^2 = m_4^2 - m_1^2$, but for large values of m_4, $m_1 \approx m_2 \approx m_3$. Finally, L is the travel distance of the neutrino of energy E_ν. We will often use this formalism to demonstrate the reach of the proposed experimental program.

Given the importance of such a sterile neutrino discovery, it is clear that the existing anomalies must be explored further by repeating the existing measurements in an effective way capable of addressing the oscillation hypothesis.

III. OPTIMIZATION STRATEGY

In this status report, we present a study of physics sensitivities focused on optimizing the configuration of the SBN program. With the MicroBooNE detector location fixed at 470 m, we focus the analysis first on determining the optimal location of the LAr1-ND detector in combination with the ICARUS T600 detector located at 600 m along the Booster Nuetrino Beam.
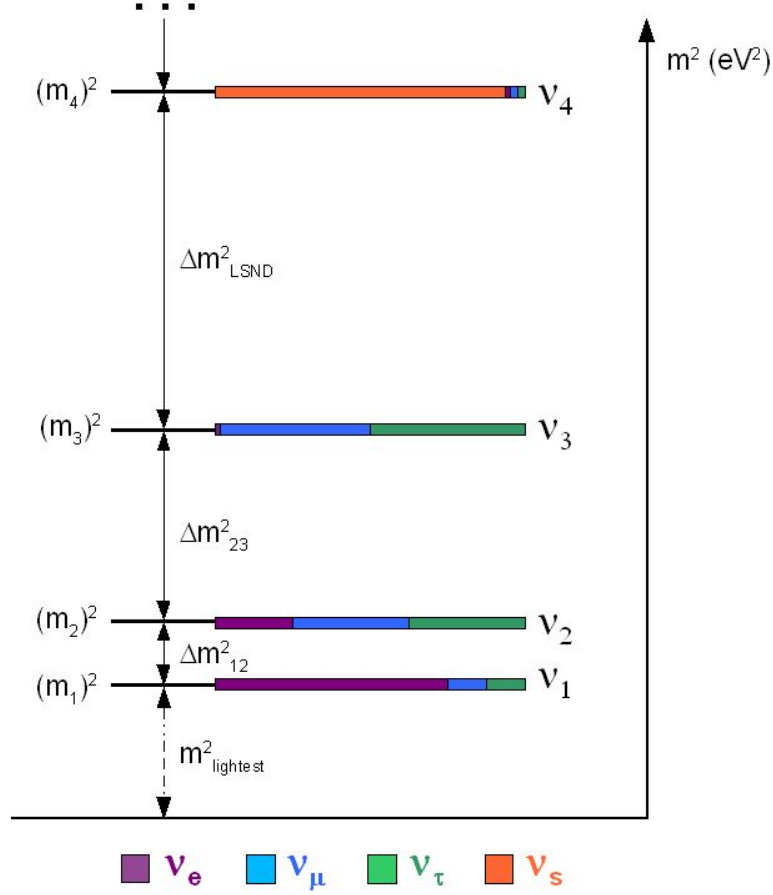
FIG. 5: *Possible hierarchy of neutrino masses with 3 active and 1 (or more) mostly sterile neutrino mass states. The LSND and other anomalous results are often interpreted as evidence for an order 1 eV^2 neutrino state that is mostly sterile.*

The experimental sensitivity to neutrino oscillation signals is determined by the statistical precision of the signal sample and the impact of systematic uncertainties associated with neutrino fluxes, neutrino interaction cross sections, and detector-related effects. The studies presented in Sections III B and III C take into account all known systematic uncertainties related to the neutrino flux predictions in a detailed way in order to optimize the detector configuration for maximal sensitivity to appearance and disappearance signals in the 0.1–10 eV^2 mass-splitting range. Both cross section and detector systematics warrant careful study, but (i) are minimized by utilizing the same nuclear target (LAr) and the same detection technique (TPC) in all detectors, and (ii) do not directly impact the optimal configuration of the experimental program regarding detector positions along the Booster Neutrino Beam. In this report, therefore, we will focus on relative comparisons of sensitivity to answer important questions about the layout of the experimental program while work continues on other aspects of the analyses.

Other important aspects, such as cosmogenic backgrounds to the ν_e event samples are also

discussed, but not yet incorporated into full physics sensitivities. We present a study of certain cosmogenic backgrounds which is used to determine the need for locating the detectors in a pit with overburden.

A. Flux Systematics

To study the impact of flux uncertainties on the oscillation searches, we take advantage of the advanced Booster Neutrino Beam (BNB) simulation code and error matrix techniques developed by the MiniBooNE collaboration and adapted by the LAr1-ND collaboration in development of their proposal. The MiniBooNE framework accounts for systematic variations in charged pion production in the target (constrained by HARP data), charged and neutral kaon production (constrained by global fits to kaon production measurements and constraints from SciBooNE), hadron re-interactions in the target, horn or other materials, and focusing effects (horn current, skin depth).

To estimate uncertainties on the nominal neutrino event predictions, the sources of systematic uncertainty are individually varied and each event in the nominal distributions are assigned a weight corresponding to its probability to exist in each different "universe". The number of events in the nominal, or *central value*, distribution is denoted as N_{CV}^i, where the index i runs across each energy bin in each detector. Drawing randomly from the allowed underlying parameters a large number of times, $\mathcal{N}$, we can construct an envelope of possible universes around the nominal prediction. The number of events in each of these systematic variations is then given as $N_{\alpha,m}^i$, where α is each systematic variation, and m is the "draw" used (chosen from $[1, \mathcal{N}]$). For each systematic error source, we then build a covariance matrix which contains both the systematic effect of each variation and, importantly, the bin-to-bin and detector-to-detector correlations. The covariance matrix for the αth systematic source is defined as:

$$E_{ij}^\alpha = \frac{1}{\mathcal{N}} \sum_{m=1}^{\mathcal{N}} [N_{\text{CV}}^i - N_{\alpha,m}^i] \times [N_{\text{CV}}^j - N_{\alpha,m}^j]. \tag{2}$$

If the underlying sources of uncertainty are taken as uncorrelated, then the total systematic error matrix is given by $E_{ij}^{syst} = \sum_\alpha E_{ij}^\alpha$.

The event rates at different detector locations will be highly correlated with regard to flux sources and we can exploit these correlations to minimize systematic uncertainties in the event rate prediction at the far detector. The scale of the correlations are influenced by both the relative location of the detectors and the angle of the beam subtended by each. Specifically, we will consider the optimal location of the near detector somewhere in the range 100-200 m from the BNB target.

Figure 6 shows an example of the flux correlation matrix ($\rho_{ij} = E_{ij}/(\sqrt{E_{ii}}\sqrt{E_{jj}})$) between the ν_μ charged-current event samples in LAr1-ND at 100 m and the T600 at 600 m on the beam axis. In the figure, each bin in the 2D histogram represents an energy bin in the reconstructed ν_μ event sample in the near detector (the first 19 bins) or the far detector (the second 19

bins). The upper-left and lower-right blocks of the matrix, therefore, indicate the high level of correlation between the ν_μ samples of the near and far detectors. This correlation is exploited in the fit for oscillation signals through the calculation of the χ^2 between the observed event rate and the prediction for a given signal, $N_{pred}(\Delta m^2, \sin^2 2\theta) = N_{CV} + N_{osc}(\Delta m^2, \sin^2 2\theta)$, using:

$$\chi^2 = \sum_{i,j} [N_{obs}^i - N_{pred}^i(\Delta m^2, \sin^2 2\theta)] \ E_{ij}^{-1} \ [N_{obs}^j - N_{pred}^j(\Delta m^2, \sin^2 2\theta)]. \tag{3}$$

where the total error matrix now contains also a contribution from statistical uncertainties, $E_{ij} = E_{ij}^{syst} + E_{ij}^{stat}$. Equation 3 allows us to build a χ^2 surface from which confidence level (C.L.) contours can be defined by relative changes in the χ^2 statistic, or $\Delta\chi^2$. In the studies presented here, however, we will focus on relative comparisons between such C.L. contours extracted from different χ^2 surfaces instead of absolute confidence limits.
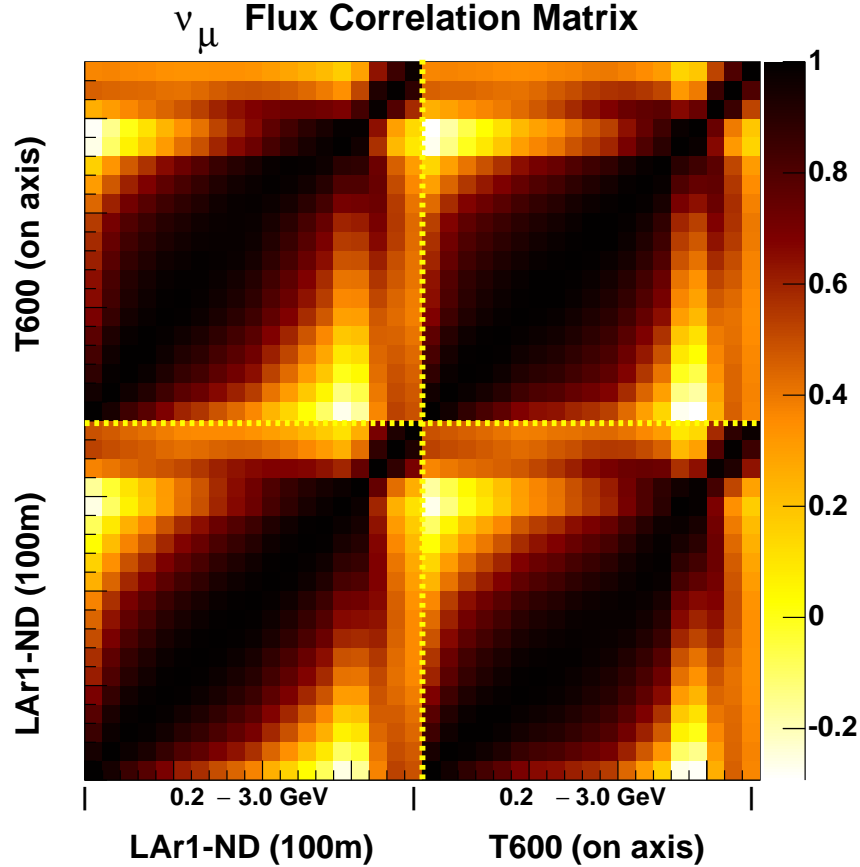

FIG. 6: *The correlation matrix between the ν_μ charged-current event samples in LAr1-ND at 100 m and the T600 detector at 600 m on-axis which shows that there are large correlations between the two detector locations.*

B.   Impact of Detector Locations on $\nu_\mu \to \nu_e$ Appearance

In order to move forward with important civil and infrastructure design considerations for the near detector, it is important to determine the optimal near detector location for the physics program. To study the impact of the SBN near detector location on the oscillation sensitivities, events were simulated using the Booster Neutrino Beam Monte Carlo and liquid argon geometries of the proper dimensions for the LAr1-ND and ICARUS detectors. The ND was simulated at 100 m, 150 m, and 200 m from the BNB target while the T600 position was fixed at 600 m.

The electron neutrino event candidate distributions in each detector are estimated by considering intrinsic ν_e charged-current (CC) interactions as well as possible beam-related mis-identification backgrounds. In this study, which is focused on the optimization of detector locations along the beam, we do not yet consider cosmogenic background sources. These will be discussed in Section III E. The event selection criteria are given below and are applied identically to both detector geometries. It is important to note that while changes in these assumptions could impact the absolute sensitivities, they should not impact these comparisons or any conclusions drawn from this study regarding the detector position.

- **ν_e CC :** Electron neutrino charged-current interactions occurring within the fiducial volume are accepted with an assumed 80% identification efficiency. The absolute efficiency will depend on the final event selections for example to address cosmogenic photon backgrounds (see Section III E). Detailed studies of event selection and efficiency are on-going.

- **NC π^0 production :** Neutral-current interactions with any number of π^0 in the final state are considered as possible background events. If more than one photon converts within the fiducial volume, the event is not considered as background. For events where only one photon converts within the fiducial volume, a 94% photon rejection rate is applied (corresponding to the expected efficiency of applying dE/dx separation of e/γ showers in the LAr TPC). Note that further rejection of this class of events is likely possible by identifying the low-energy hadronic debris near the vertex of the neutral-current interaction. The electromagnetic shower produced by the photon will be separated from, but point back to, this vertex. An observed gap between the photon shower and the interaction vertex would allow further rejection of single photon neutral-current events.

- **NC γ production :** Neutral-current interactions resulting in photons in the final state (not from π^0 decays) are also considered as background if the photon converts within the fiducial volume and 6% of these events are accepted into the ν_e candidate sample (corresponding to the expected efficiency of applying dE/dx separation of e/γ showers in the LAr TPC). Just as in the photon production from π^0 described above, there is the additional possibility to reject these events through the identification of a separated interaction vertex which is not being utilized here.
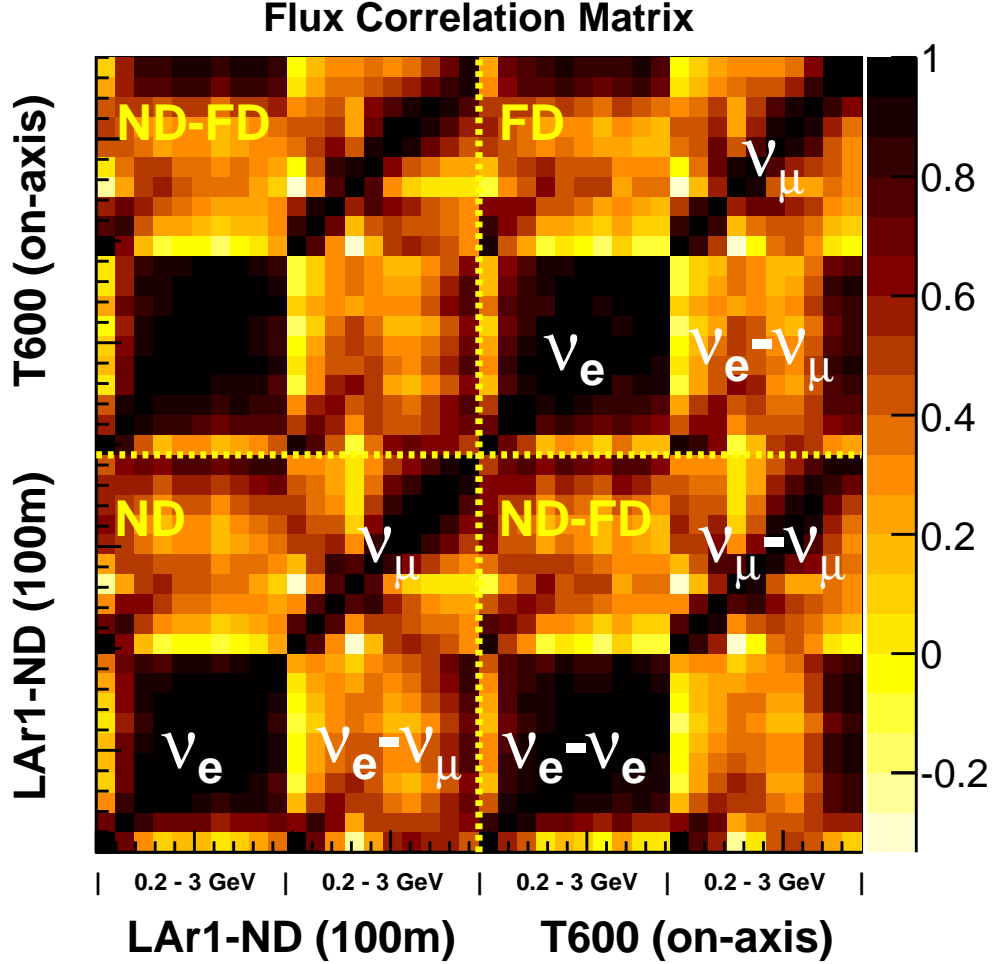
Flux Correlation Matrix

FIG. 7: *The correlation matrix between the ν_e and ν_μ event samples in the near and far SBN detectors which shows the large correlations between the two detector locations but also between the two event samples within a single detector.*

- ν_μ **CC** : ν_μ charged current interactions in the presence of an identified primary e.m. shower within the fiducial volume could be mis-identified as electron neutrino interactions if the muon is not identified.

By analyzing the conversion points of photons instead of the true neutrino interaction vertex, we accurately account for acceptance effects in the differently shaped detectors. Because the e/γ separation is performed entirely with the first few centimeters of a shower, differences in total shower containment do not affect the assumption that the photon identification efficiency is the same in each detector.

Figure 7 shows the full correlation matrix generated from the underlying flux-related systematic variations for the ν_μ and ν_e charged-current event samples in the LAr1-ND detector
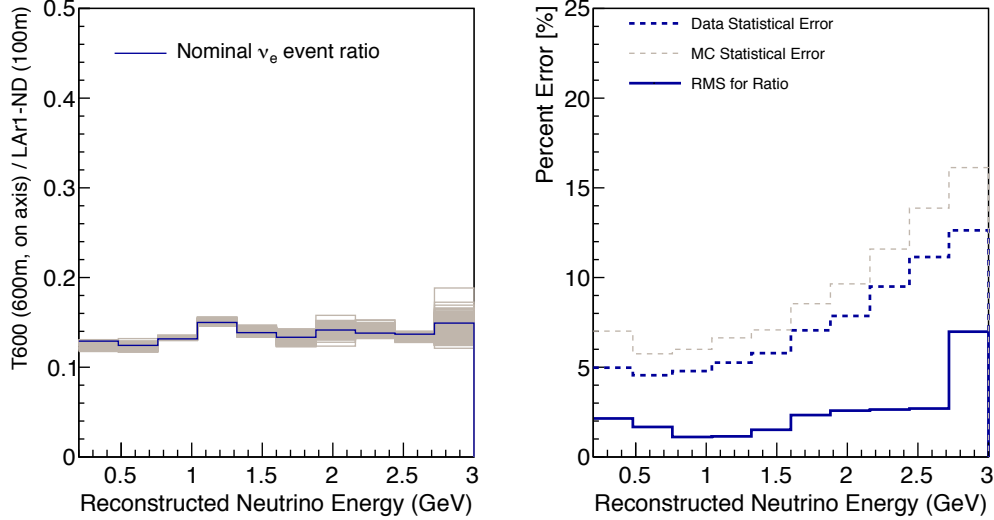
FIG. 8: *Left: Ratio of the ν_e-CC event candidate rates in the T600 detector (on-axis at 600 m) to that in LAr1-ND at 100 m. The blue line is the nominal flux ratio, while the grey band is the flux-related systematic variations around this nominal expectation. All flux-related systematics in the BNB simulation are considered including π, K production, hadron reinteractions, and horn focusing. Right: The blue line shows the RMS spread of the systematic variations around the mean of the ratio curves, in percent. The blue dashed line shows the expected data statistical errors for a nominal run for comparison. The MC statistical errors used in the present analysis are indicated as well. A roughly data-sized MC sample was generated for the analysis. These uncertainties have been estimated using the LAr1-ND simulation and analysis tools and the MiniBooNE BNB simulation software.*

at 100 m and the T600 detector at 600 m on-axis. In this rather complicated plot we observe several key features. First, the ν_e event distributions within a single detector are highly correlated. The uncertainties tend to move the full event spectrum up and down together. Second, the ν_e event rates in the ND-FD are also very highly correlated (this is the block labeled ν_e–ν_e), suggesting that the observed ν_e sample in the ND will provide a powerful constraint of the prediction in the FD. Finally, we see that the ν_μ and ν_e samples are also moderately correlated.

Figure 8 shows the ratio of the nominal ν_e charged-current event candidate distributions in the ICARUS and LAr1-ND detectors along with the flux-related systematic uncertainties on that ratio. The RMS (in percent) of the varied "universes" is shown as well as the expected statistical uncertainties for a nominal 6.6×10^{20} p.o.t. run. This ratio is illustrative for understanding the cancellation of systematic uncertainties that is enabled in a multi-detector analysis. The RMS variation in the FD/ND event ratio is 2-3% at all neutrino energies except the very high-energy tail of the event distribution. Note this is well below the expected
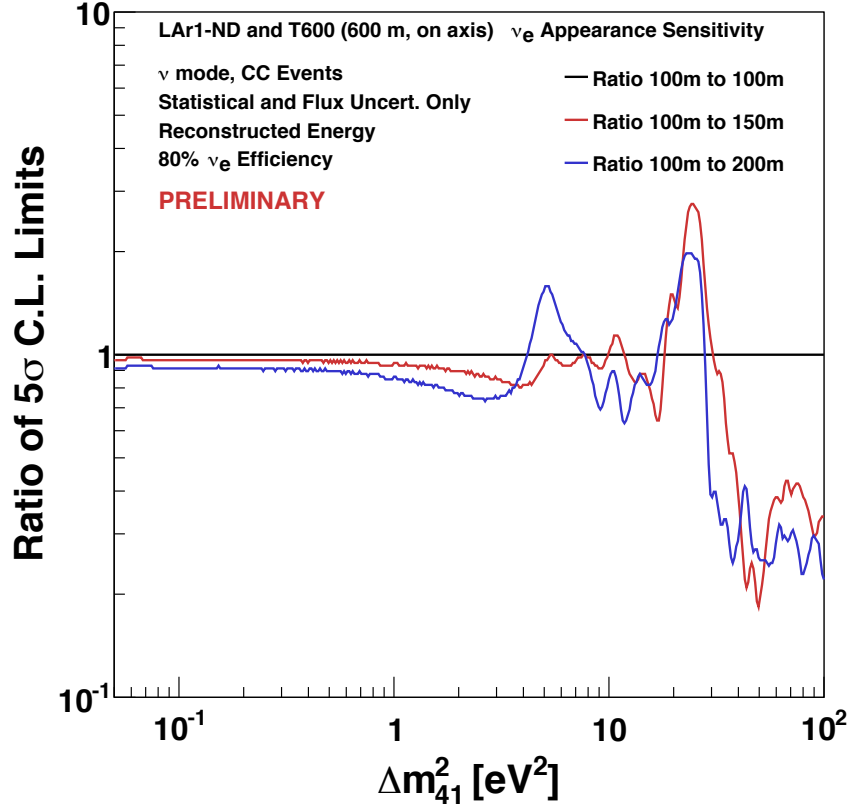
FIG. 9: *Comparison of the 5σ confidence level ν_e appearance sensitivity contours for three different positions of the near detector, LAr1-ND (100 m, 150 m, 200 m). Each curve is constructed by dividing the $\sin^2(2\theta)$ value that sits on the 5σ (or $\Delta\chi^2 = 25$) contour at a particular value of Δm^2 for the 100 m configuration, which serves as a reference, by the corresponding value from the other experimental configurations. Values below 1.0 indicate less coverage at that confidence level than the 100 m configuration, whereas values above 1.0 indicate better sensitivity at that Δm^2.*

statistical uncertainties for this event selection.

Figure 9 compares directly the resulting oscillation sensitivities for the three simulated positions of the near detector (100 m, 150 m, 200 m). The comparison is done by taking the ratio of the $\sin^2(2\theta)$ value that sits on the 5σ confidence level sensitivity contour at each Δm^2 for the 100 m configuration, which serves as a reference, to the same value for the 150 m and 200 m configurations. Therefore, values below 1.0 on the curves indicate less coverage at that confidence level than the 100 m configuration, whereas values above 1.0 indicate better sensitivity at that Δm^2. The sensitivities are comparable, though the ND located near 100 m performs slightly better at most values of Δm^2. The reduction in sensitivity for more distant ND positions is largely due to the presence of appearance signal in the near detector, which gets normalized out in the analysis and tends to shrink the excess observed in the far detector.

Our analysis indicates that any small increase in the correlations between the neutrino fluxes at the ND and FD locations does not outweight the disadvantage of reduced ND statistics and the presence of oscillation signal in the ND sample. Given this result and the cost advantage to using the SciBooNE enclosure to house the cryogenic system for the LAr1-ND experiment, a near detector location near 100 m appears optimal.

C.   Impact of Detector Locations on ν_μ Disappearance

An observation of ν_e appearance that is to be interpreted as an oscillation signal should be accompanied by the disappearance of ν_μ with equal or greater probability. A sensitive search for ν_μ disappearance is an important component of the test for low-mass sterile neutrinos.

To assess the impact of the near detector location on the sensitivity to ν_μ disappearance, we follow the same analysis as for ν_e appearance. ν_μ charged-current interactions are selected with an assumed 80% efficiency. For now, we do not consider neutral current charged pion backgrounds. Detailed studies of the event selection and efficiency are required before the absolute sensitivity can be established.

Figure 10 shows the ratio of the nominal ν_μ charged-current event candidate distributions in the ICARUS T600 detector at 600 m to that in LAr1-ND at 100 m along with the flux-related systematic variations on the ratio. The RMS (in percent) of the varied "universes" is also shown along with the expected statistical uncertainties for a nominal run of the SBN program of 6.6×10^{20} p.o.t. This ratio is valuable for understanding the scale of the cancellation of flux-related systematic uncertainties in a muon neutrino disappearance search.

Figure 11 compares directly the resulting ν_μ disappearance oscillation sensitivities for the three simulated positions of the near detector (100 m, 150 m, 200 m). As with ν_e appearance, the ND located near 100 m performs better at most values of Δm^2. There are significantly larger statistical samples in a nearer detector (a factor 4.4 between 100 m and 200 m, for example), which has some impact on the ν_μ disappearance analysis but is also very important for other aspects of the physics program, such as precision cross section measurements. Therefore, the conclusion is again that a near detector location near 100 m appears optimal.

D.   Other Systematics

Additional systematic uncertainties could arise from differences in the responses of the neutrino detectors. In the SBN multi-detector LAr TPC program, detector systematics can be relevant only if there are important differences in efficiencies or physical differences between the near and far detectors. Differences can arise from:

- LAr purity levels. The goal is to design cryostat and cryogenic systems for very high LAr purity to increase electron lifetimes to permit long drift distances with the highest signal quality. Specific requirements remain to be defined. For example, 5 ms electron lifetime
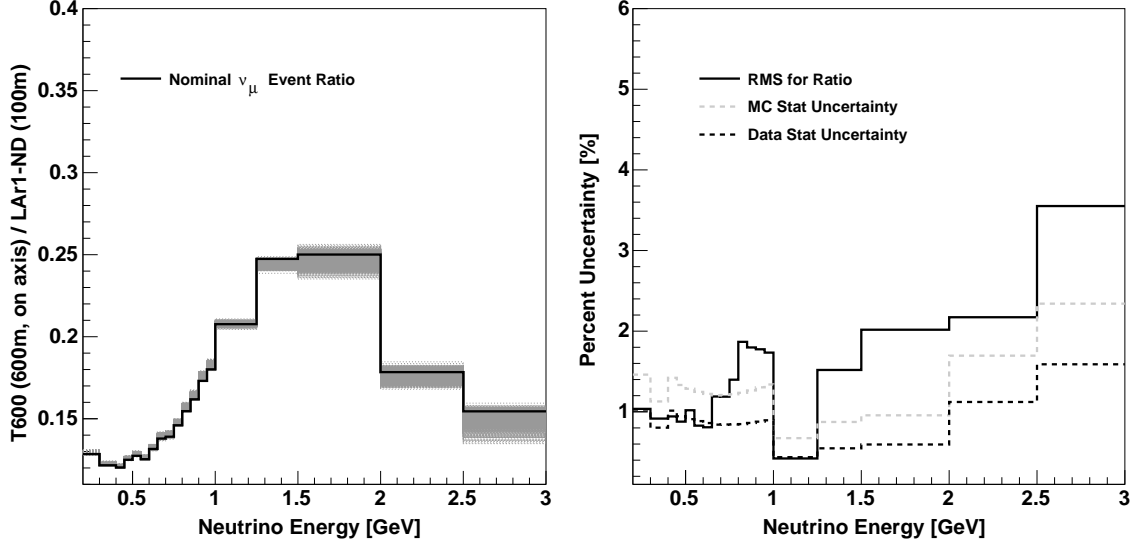
FIG. 10: *Left: Ratio of the ν_μ-CC event rate observed in the T600 detector (on-axis at 600 m) and in LAr1-ND (at 100 m). The black lines are the nominal flux ratio, while the grey bands are the flux-related systematic variations around this central value expectation. All flux-related systematics in the BNB MC are considered including π, K production, hadron reinteractions and horn focusing. Right: The black lines show the RMS spread of the systematic variations around the mean of all the ratio curves, in percent. The green dashed lines show the expected data statistical errors for a nominal run for comparison. The MC statistical errors are also indicated, which explain any fluctuations in the nominal ratios on the left. These uncertainties have been estimated using the LAr1-ND simulation and analysis tools and the MiniBooNE BNB simulation software.*

leads to 20% attenuation over 2 m. Continuous monitoring of the electron lifetime during detector operation is very important;

- Efficiencies of the light collection systems used to identify off-beam interactions by time and to remove backgrounds;

- Electric drift fields and their homogeneity. UV laser calibration can be used for field corrections.

- Geometrical differences, like different stereo angle of the wires and wire pitch. Wire spacing determines the detector resolution (smaller wire spacing leads to higher resolution and better particle ID). The three SBN detectors have all the same (3 mm) wire spacing.

- Electronic readout: shaping, sampling time, signal/noise ratios, general noise conditions affecting the identification/measurement efficiencies. The use of cold electronics reduces cable length and improves signal/noise.
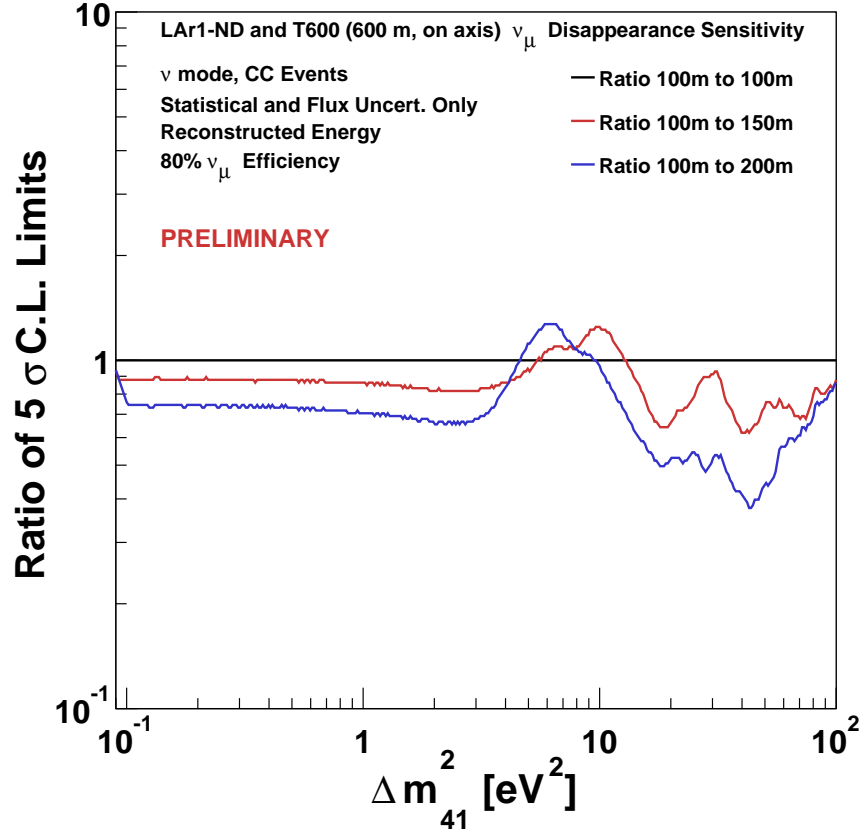
FIG. 11: *Comparison of the 5σ confidence level ν_μ disappearance sensitivity contours for three different positions of the near detector, LAr1-ND (100 m, 150 m, 200 m). Each curve is constructed by dividing the $\sin^2(2\theta)$ value that sits on the 5σ (or $\Delta\chi^2 = 25$) contour at a particular value of Δm^2 for the 100 m configuration, which serves as a reference, by the corresponding value from the other experimental configurations. Values below 1.0 indicate less coverage at that confidence level than the 100 m configuration, whereas values above 1.0 indicate better sensitivity at that Δm^2.*

Moreover, it is important to know the effects induced by the different rates at the two sites, like different background levels from cosmic rays (see Section III E) and beam dirt events as well as effects due to different aspect ratios of the near and far detectors through possible variations of acceptance and efficiency.

The near and far detectors will be carefully designed to meet the requirements and reduce possible systematics effects. The energy calibration and detector inter-calibration can be done as far as is possible with external datasets (for example, neutrino-induced through-going muons, cosmic events and π^0 mass measurements). Overall, typical detector uncertainties are smaller than flux and cross section uncertainties, with values of a few percent.

E.   Cosmic Backgrounds

An important background to consider for the ν_e appearance channel is cosmogenic photons that generate electrons in the detector via Compton scattering or pair production misidentified as a single electron. Compton scattering in this relativistic limit ($E_\gamma/m_e >> 1$) gives, with high probability, a very forward electron carrying almost all the energy of the gamma. Understanding the scale of this background is critical to establishing the configuration of the SBN program since background mitigation could require overburden for the detectors and/or selection cuts that reduce the efficiency of ν_e reconstruction.

For the following analysis, only those backgrounds in the beam spill time (1.6μs) rather than the drift time ($\sim$1ms) are counted. The impact of cosmics collected in the drift time has to be carefully addressed in order to reach the necessary large rejection factor for particles out of spill.

Several independent determinations of the cosmic flux were evaluated at the surface and at shallow depth using simulations developed by the MicroBooNE, LBNE [14], and ICARUS collaborations. The MicroBooNE simulations were performed with the CRY cosmic-ray shower simulation [15] as a primary particle generator. LBNE have used CRY for atmospheric protons, neutrons and photons, and the modified Gaisser's parameterization for atmospheric muons. The ICARUS collaboration have used FLUKA [16]. The simulations were compared to other cosmic ray generators and measurements by the groups performing them but these comparisons are not discussed further here. Results presented here are based on truth tables from the simulation in all cases. The results of the LBNE simulations were extrapolated to the Fermilab site and comparisons were made between the simulations by scaling to common surface areas.

The simulations made for three different detectors are compared by scaling the rates based on the surface area of the detector. Scaling by surface area is conservative in that it allows for the appropriate edge cosmogenic production, but over-scales the volume effects like secondary production and general containment of the background. A detailed simulation will likely reveal a scaling factor that is intermediate between the two.

The MicroBooNE study is based on a detector on the surface with no overburden. The LBNE studies are based on a detector in a pit at a depth similar to the BNB beamline and with a 3 m rock (8.1 m w. e.) overburden. For ICARUS two configurations were studied: a surface detector with no overburden and a detector in a pit with the detector on the BNB beamline and a 3m overburden.

The simulations show reasonable agreement on the flux of cosmogenic particles at the surface. For example, the first row of Table II lists the rate of photons above 1 GeV at the surface. The CRY simulations by MicroBooNE and LBNE are in complete agreement while the ICARUS rate is about a factor of two higher. Similar agreement is seen in the rates of muons and hadrons.

The following comparisons are based on propagating generated the particles (proton, muons, photons, etc) through any overburden into the detectors where hit rates are estimated. Particle rates in the detectors are converted into counts using an integrated exposure time of 210 sec-

	Detector	MicroBooNE	ICARUS		LBNE	LAr1-ND
1	Cosmic γ Rate	$0.332\mathrm{m}^{-2}\mathrm{s}^{-1}$	$0.75\ \mathrm{m}^{-2}\mathrm{s}^{-1}$		$0.331\mathrm{m}^{-2}\mathrm{s}^{-1}$	
2	Active mass	89t	Scaled by area to MicroBooNE	475t	Scaled by area to MicroBooNE	82t
3	Surface (w/o bottom)	87.5 m^2	87.5 m^2	289 m^2	87.5 m^2	75.8 m^2
4	N_γ(E$_\gamma$ > 200 MeV), w/o OVB	31680	43296	143000		
5	N_{Compton}(E > 200 MeV), w/o OVB	634	1449	4787		549
6	N_γ(E$_\gamma$ > 200 MeV), w/ OVB		15986	52800	4576 (E> 250 MeV)	
7	N_{Compton}(E > 200 MeV), w/ OVB		490	1619	137	
8	N_e(Intrinsic ν_e CC, E > 0 MeV)	567		2000		17649

TABLE II: *Summary of estimated cosmogenic photon background faking electrons in the three SBN detectors. To provide a basis for comparison, the rates in the ICARUS detector are also provided scaled by area to the size of MicroBooNE. Rates estimated for an LBNE detector in a shallow pit are also given scaled to the size of MicroBooNE and the elevation of Fermilab. The photon and electron counts represent 210s of integrated beam spill time (6.6E20 p.o.t.). The intrinsic ν_e is based on 6.6E20 p.o.t. Labels "w/OVB" and "w/o OVB" represent with 3m overburden and detectors in a pit and without overburden at surface, respectively.*

onds, corresponding to the integrated spill exposure for 6.6×10^{20} protons on target. To allow a validating comparison of the simulations, the ICARUS and LBNE numbers are scaled by detector surface area (not volume) exposed to the photons. In Table II both the scaled (column 3) and un-scaled (column 4) numbers are shown for ICARUS while only the scaled numbers are shown for LBNE. The 3rd row of the table lists the surface areas used for scaling.

The 4th row of the table list the number of photons with E>200 MeV for a surface detector. The 6th row shows the same number for detectors in a pit with overburden (the LBNE analysis uses a 250 MeV cut). The 5th and 7th rows of the table list the number of Compton electrons for the surface and pit configurations respectively. Row 8 lists the intrinsic ν_e background for each detector volume and location.

In the MicroBooNE study, a simulation was performed to estimate the interactions of the photons generating electrons. Comparing the rates of Compton electrons for a surface detector (row 5), the scaled ICARUS result is about a factor two higher than MicroBooNE. Some of this difference may be due to the scaling procedure. The MicroBooNE result is at the same scale as the intrinsic ν_e background from the beam while the ICARUS result is a factor 2.5 higher.

Placing T600 at shallow depth and with an overburden, the rate of Compton electrons is reduced by a factor of 3 as shown in the Table. This rate is then comparable to the intrinsic ν_e background. For these cosmogenic rates no further cuts are applied to remove events where the cosmic activity (e.g. muon) that generates the photon is visible in the detector. Such cuts and their rejection power and efficiency will be studied.

A comparison of the LBNE and ICARUS simulations is made using the numbers scaled by area to the MicroBooNE size. In the LBNE analysis a 3% factor for photons producing a Compton electron in argon at 250 MeV was used. The scaled ICARUS rates are 3.5 times the scaled LBNE rates. The LBNE electron background beneath 3 m of rock is dominated by photons produced by atmospheric muons. In LBNE simulations, secondary photons in a cascade produced by electrons are not counted since the cascade was assumed to be initiated by the 'primary' electron. Counting all photons in the cascades with the same threshold, would increase the total number of photons by a factor of 1.6.

The intrinsic ν_e CC rate from beam in the LAr1-ND detector will be much larger than cosmogenic induced Compton electrons while for MicroBooNE and ICARUS the cosmogenic Compton electrons are similar to the expected intrinsic ν_e CC from the beam. We use the estimates for the detectors in a pit and with overburden as a baseline for this comparison and note that the background increases significantly at the surface without overburden. A study from LBNE shows that 3 m of rock suppresses muon fluxes by about a factor of 2 (on top of the detector) but the fluxes of atmospheric neutrons and protons are suppressed significantly (by factors up to 5-10) by 1 m of rock. Atmospheric photons are attenuated even more. Thus 3 m of rock will get rid of most of this background leaving muon-induced photons as the most important one.

We have not considered here the contribution of pair production, where one electron (or positron) is lost. The LBNE study shows that the rates are similar, i.e. several percent, to the rate of Compton scattering at low energy (100 MeV). This allows us to compare the numbers in Table II. The total cosmogenic induced electron events before applying cuts can go up by a factor of two to three due to this. A higher energy threshold would extinguish the Compton scattering rate with the cosmogenic electron rates then driven by the mis-identification pair production. To evaluate the rate coming from mis-identification, reconstruction cuts need to be applied that will also affect the signal. This level of study has not been completed.

The numbers shown in Table II are calculated within the spill time (1.6μsec) and not integrating over the full drift time ($\sim$1 ms). The planned light detection systems for both the near and far detectors will be critical to achieving the rejection factor implied by this assumption. This assumption neglects pile-up of cosmogenic electron events with other cosmogenic events (like muons) or overlap with e.g. a ν_μ NC interaction in the beam window. We note, nevertheless, that systems and components to mitigate also other cosmogenic sources (muon veto, photon detection systems) could play an important role.

There are several options to address the cosmogenic backgrounds at the SBN program at Fermilab. Locating the detectors underground with over burden reduces the rates. The configuration for the program described in Section IV assumes the detectors will located in a pit with the capability of at least 3m overburden. Furthermore, the possibility of an active veto, probably using plastic scintillator, is being considered. Finally, event selection cuts will be developed to further reduce this background component. For example, LBNE studies have shown that cuts on accompanying muons or other activity around the electron can be very effective. Although preliminary studies of event selection and efficiency for the ICARUS detector have

started, optimization will require a more detailed and complete analysis in order to determine the detection efficiency in the presence of external background sources. For instance, additional selection criteria required to reduce the photon background events entering from the detector sides are expected to further reduce the quoted electron recognition efficiency. These analyses are not yet mature, so we do not attempt to make projections on the experiment sensitivity at this time.

F.   Neutrino Cross Sections and the MiniBooNE Low-Energy Excess

Precise cross section measurements are considered a fundamental prerequisite for every neutrino oscillation study. In the energy range of interest, multiple possible interaction processes (quasi-elastic, resonances, DIS) and complicated nuclear effects in neutrino interactions on argon result in a variety of final states. These can range from the emission of multiple nucleons to more complex topologies with multiple pions, all in addition to the leading lepton in CC events. Liquid argon TPC technology is particularly well suited to this purpose because of its excellent particle identification capability and calorimetric energy reconstruction down to very low thresholds.

LAr1-ND provides an ideal venue to conduct precision cross section measurements in the critical 1 GeV range. Due to its location near the neutrino source and relatively large mass, the near detector will make measurements of neutrino interactions with high statistics ($\sim$1M events per 2.2×10^{20} POT). Full details of the expected event counts are available in the original LAr1-ND proposal submitted to the PAC in January, 2014.

Another critical aspect of the LAr1-ND physics program is the resolution of the anomalous event excess reported by MiniBooNE described in Section II. Regardless of what MicroBooNE determines as the nature of the MiniBooNE excess, electrons or photons, a near detector is needed to understand if the effect appears over a distance or exists intrinsically in the beam. LAr1-ND, sited at 100 m, can address this important question with high significance in a relatively short run.

In the case that MicroBooNE determines the observed MiniBooNE excess to be events with single photons in the final state, only a few dozen events above expected backgrounds at low-energy are expected. In this scenario, LAr1-ND can quickly confirm whether the effect is intrinsic in the beam (i.e. that it is most likely some standard, but un-modeled neutral-current interaction), and would then expect to observe hundreds of events per year. Such a sample will enable a measurement of this reaction with much greater precision and inform the development of cross section models to include this process with the correct rate. This will be important input for some accelerator-based neutrino experiments studying oscillations at the atmospheric Δm^2 that observe signals in the few hundred MeV energy range. In particular, a new source of single photon final states has implications for other Cerenkov detector neutrino experiments in the same energy range, such as T2K.

The siting near 100 m, providing an increase in statistics of 2-5$\times$ over the other options, is

clearly the most optimal of the three considered locations for these aspects of the SBN physics program.

IV.   REFERENCE PROGRAM CONFIGURATION

To accomplish this physics program, the future short-baseline experimental configuration is proposed to include three LAr TPCs located on-axis in the Booster Neutrino Beam as summarized in Table III. The near detector (LAr1-ND) will be located in a new enclosure directly downstream of the existing SciBooNE enclosure. The MicroBooNE detector, which is currently in the final stages of installation, is located in the Liquid Argon Test Facility (LArTF). The far detector (T600) will be located in another new building between MiniBooNE and the NOvA near detector surface building. Figure 12 shows the locations of the detectors superimposed on an aerial view of the Fermilab neutrino experimental area. The following sections describe the attributes of the three detectors, work on common cryogenic systems, and civil construction. The initial physics studies are all based on the assumption that no modifications will be made to the BNB target and horn. However, studies have been initiated to determine what changes could be made to the target and horn to re-optimize for a BNB program based on LAr TPC detectors rather than the MiniBooNE Cerenkov detector.

Detector	Distance from BNB Target	LAr Total Mass (Tons)	LAr Active Mass (Tons)
LAr1-ND	110 m	180	82
MicroBooNE	470 m	170	89
T600	600 m	760	476

TABLE III: *Summary of the SBN LAr TPC detector locations and masses.*

A.   Near Detector: LAr1-ND

The design of the LAr1-ND detector [2] builds on many years of LAr TPC detector R&D and experience from design and construction of the ICARUS T600, ArgoNeuT, MicroBooNE, and LBNF detectors. The basic concept is to construct a membrane-style cryostat at 110 m from the Booster neutrino source in a new on-axis enclosure adjacent to and directly downstream of the existing SciBooNE hall (Figure 13). The membrane cryostat will house a CPA (Cathode Plane Assembly) and multiple APAs (Anode Plane Assemblies) to read out ionization electron signals. The two APAs located near the beam-left and beam-right walls of the cryostat will each hold 3 planes of wires with 3 mm wire spacing. The APA uses the same wire bonding method developed for the LBNF APAs, but without the continuous helical wrapping to avoid ambiguity in track reconstruction. The wire readout arrangement is identical to MicroBooNE,
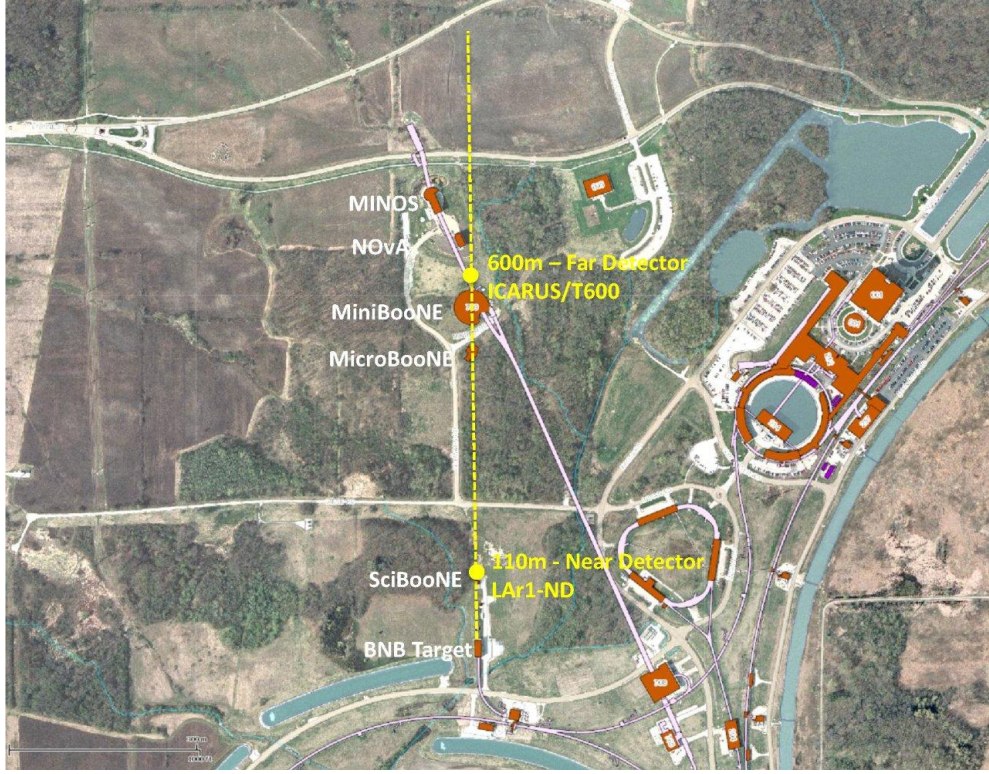
FIG. 12: *Map of the Fermilab neutrino beamline area showing the axis of the BNB (yellow dashed line) and approximate locations of the SBN detectors at 110 m, 470 m, and 600 m. The pink line indicates the axis of the NuMI neutrino beam for reference.*

with banks of cold electronics boards at the top and two vertical sides of each APA. The total number of readout channels is 4,736 per APA (9,472 in the entire detector). The CPA has the same dimensions as the APAs and is centered between them. It is made of a stainless-steel framework, with an array of stainless-steel sheets mounted over the frame openings. Each pair of facing CPA and APA hence forms an electron-drift region. The open sides between each APA and the CPA are surrounded by 4 FCA modules, constructed from FR4 printed circuit panels with parallel copper strips, to create a uniform drift field. The drift distance between each APA and the CPA is 2 m such that the cathode plane will need to be biased at $\sim$100 kV. The active volume, determined by the size of the anode wire plane and cathode assemblies, is 4.0 m (width) $\times$ 4.0 m (height) $\times$ 3.65 m (length) containing 82 tons of liquid argon (Figure 13). The LAr1-ND design will additionally include a light collection system using a compact light-guide-based system for detecting scintillation light similar to the one being proposed for LBNF. The necessary cryogenics system will be described in Section IV D. In addition, we are looking into the possibility of placing shielding over the near detector should it be deemed necessary to reduce cosmics. Overall, the design philosophy of the LAr1-ND detector is to serve as a prototype for LBNF that functions as a physics experiment. While the present conceptual
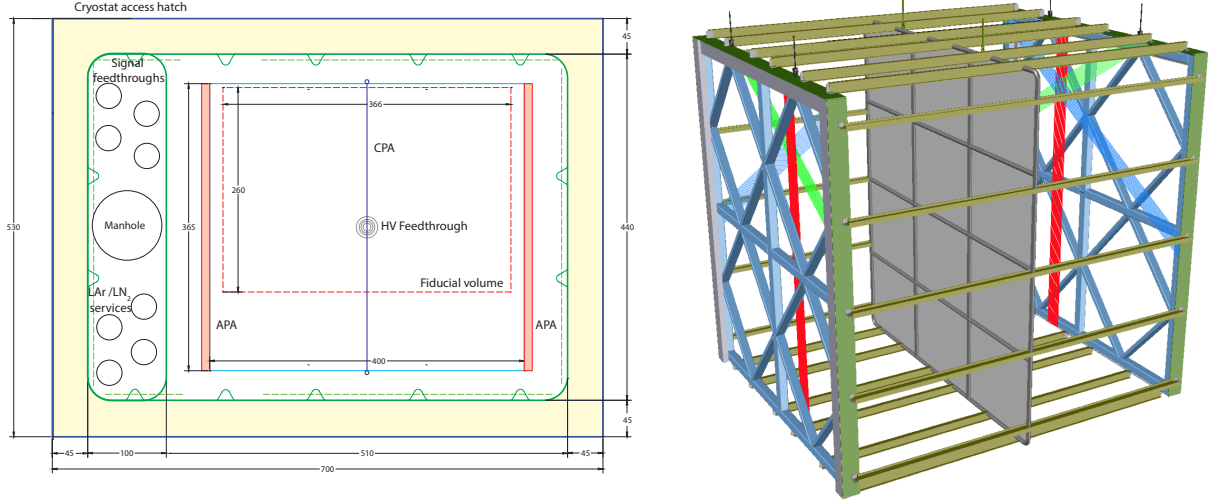
FIG. 13: *Left: Top view schematic of the LAr1-ND membrane cryostat detector concept. Foam insulation surrounds the corrugated stainless steel membrane filling the near detector enclosure. Right: Conceptual design of the LAr1-ND TPC. The total size of the TPC is 4.0 m (width) × 4.0 m (height) × 3.65 m (length) with the longest dimension along the neutrino beam direction. Note: the field cage panels are removed from view in this schematic.*

design described here is an excellent test of LBNF detector systems sited in a neutrino beam, the LAr1-ND collaboration is exploring innovations in this design and the opportunity to further test them in a running experiment.

B.   The MicroBooNE Experiment

The mid-range detector in this short-baseline configuration is MicroBooNE. MicroBooNE is currently under construction and will be commissioned at the end of this year. The experiment will measure neutrino interactions in argon for multiple reaction channels and investigate the source of the currently unexplained excess of low energy electromagnetic events observed by MiniBooNE. MicroBooNE also incorporates several important R&D features: the use of a non-evacuated cryostat, passive insulation of the cryostat and cryogenics, cold (in liquid) electronics, a long 2.56 meter drift distance, and a novel UV laser calibration system [17]. To accomplish these goals, the MicroBooNE detector is a 170 total mass (89 ton active mass) liquid argon TPC contained within a conventional cryostat [18]. The active volume of the TPC is a rectangular solid of dimensions 2.33 m × 2.56 m × 10.37 m (Figure 14). The TPC cathode plane forms the vertical boundary of the active volume on the left side of the detector when viewed along the neutrino beam direction (beam left). An array of 32 PMTs additionally line the beam
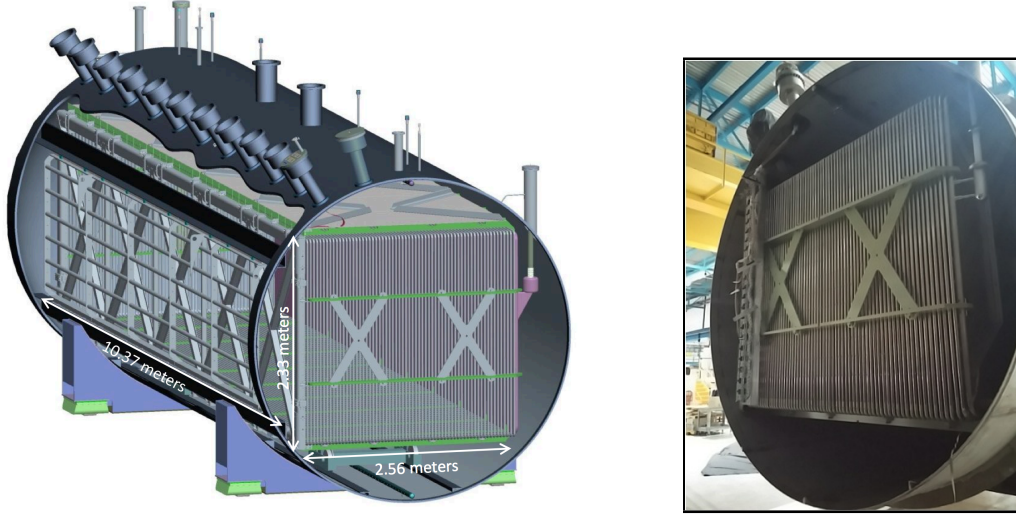
FIG. 14: *Left: The 170 ton (total mass) MicroBooNE detector as viewed from the downstream end of the vessel. The detector cryostat houses the TPC which surrounds a liquid argon volume in the shape of a rectangular box of dimensions 2.33 m (height) × 2.56 m (width) × 10.37 m (length). The mechanical structure consists of a cathode plane, field cage, wire planes, a frame for the light collection system, and G10 support beams. The cathode plane is on the right of the picture. The three readout wires planes and the light collection system consisting of 32 PMTs (not shown) are on the left. The drift distance is 2.56 meters. Right: A photograph of the completed detector right before the endcap was welded on in June 2014.*

right side of the detector to collect prompt scintillation light produced in the argon [19]. The MicroBooNE TPC design allows ionization electrons from charged particle tracks in the active liquid argon volume to drift 2.56 meters to a three-plane wire chamber. Three readout planes, spaced by 3 mm, form the beam-right side of the detector, with 3,456 Y wires arrayed vertically and 2,400 U and 2,400 V wires oriented at ±60 degrees with respect to vertical.

This detector will soon be exposed to an intense low energy neutrino source. MicroBooNE is approved to receive an exposure of 6.6×10^{20} protons on target from the existing on-axis Fermilab Booster Neutrino Beam. It will also record interactions from an off-axis component of the NuMI neutrino beam. During MicroBooNE running, the BNB will be operated in the same configuration that successfully delivered neutrino and antineutrino beam to MiniBooNE for more than a decade, thereby significantly reducing systematic uncertainties in the comparison of MicroBooNE data with that from MiniBooNE.

As of the writing of this document, construction of the MicroBooNE TPC has been completed and on June 23, 2014, the MicroBooNE vessel was moved to the Liquid Argon Test Facility (LArTF), a new Fermilab enclosure just upstream of the MiniBooNE detector hall in the Booster neutrino beamline (Figure 15). Final installation and detector commissioning has begun. MicroBooNE is on schedule to begin taking neutrino data in early 2015.

FIG. 15: *Delivery of the MicroBooNE detector to LArTF in the Fermilab BNB on June 23, 2014. The building was constructed to support the weight of additional shielding should this be deemed necessary for reducing cosmics.*

C. Far Detector: ICARUS T600

The ICARUS T600 detector installed in the underground INFN-LNGS Gran Sasso Laboratory has been the first large-mass Liquid Argon TPC (LAr-TPC) operating as a continuously sensitive general purpose observatory. The successful operation of the ICARUS T600 LAr-TPC demonstrates the enormous potential of this detection technique, addressing a wide physics program with the simultaneous exposure to the CNGS neutrino beam and cosmic-rays [20].

The ICARUS T600 detector is made of a large cryostat split into two identical, adjacent modules with internal dimensions $3.6 \times 3.9 \times 19.6$ m^3 filled with about 760 tons of ultra-pure liquid argon [20, 21]. Each module houses two TPCs separated by a common central cathode. A uniform electric field ($E_D = 500$ V/cm) is applied to the drift volume. The reliable operation of the high-voltage system has been extensively tested in the ICARUS T600 up to about twice the operating voltage (150 kV, corresponding to $E_D = 1$ kV/cm). All the detector components are held by a self-supporting low carbon stainless steel structure and thermal insulation surrounds the two cold vessels (Figure 16).

Each TPC is made of three parallel wire planes, 3 mm apart, with 3 mm pitch, facing the drift path (1.5 m). Globally, 53,248 wires with length up to 9 m are installed in the detector. By appropriate voltage biasing, the first two signal sensing planes (Induction-1 and Induction-2) provide induced signals in a non-destructive way, whereas the last Collection plane finally collects the ionization charge. On each chamber, the wire planes are oriented at 0^0, $\pm 60^0$

angles with respect to the horizontal direction. Therefore a three-dimensional image of the ionizing event is reconstructed combining the wire coordinate on each plane at a given drift time. A resolution of about 1 mm^3 is uniformly achieved over the whole active volume (340 m^3 corresponding to 476 t).

The ICARUS experiment at LNGS has now successfully completed a three year physics run from October 2010 to December 2012 in the CERN to Gran Sasso (CNGS) neutrino beam, corresponding to 8.6×10^{19} protons on target. The CNGS beam, originating at the CERN SPS, has a peak energy near 17 GeV and the baseline to Gran Sasso is 732 km. Additional data were also collected with cosmic rays to study the detector capability for atmospheric neutrinos and proton decay. From the technological point of view, the T600 run was a complete success, featuring a smooth operation, high live time, and high reliability.

Of particular interest is the search for an anomalous, LSND like appearance of ν_e in a sample of 2450 events, out of which 6 were identified as ν_e CC, consistent with the expected background from conventional sources of (7.9 ± 1.0) events. The corresponding new limits on the oscillation probability are $P(\nu_\mu \to \nu_e) = 3.8 \times 10^{-3}$ and $P(\nu_\mu \to \nu_e) = 7.6 \times 10^{-3}$ at 90% and 99% C.L., respectively [22, 23]. Further analysis of the large amount of physics data is progressing, as well as detailed evaluation of the technical aspects.

It is envisaged to move the ICARUS experimental setup to Fermilab where the ICARUS T600 detector will be operated as a far detector 600 m from the neutrino source on-axis in the Booster Neutrino Beam [1].

The ICARUS T600 detector is now in the process of being moved to CERN for a complete overhauling preserving most of the existing operational equipment, while upgrading some components with up-to-date technology in view of its future non underground operation. The refurbishing will include the following main activities:

- Realization of new vessels for LAr containment, based on aluminum extruded profiles;

- Realization of new thermal insulation, based on similar technology as foreseen for LBNE and the near detector;

- Implementation of a new light collection system, that will allow automatic event localization and disentangling from the background induced by cosmic rays;

- Implementation of new readout electronics, with new internal cabling. The possibility to insert part of the electronics in the LAr volume is presently under study;

- Complete review and maintenance of the cryogenics and purification systems (see next section).

In addition, given the latest achievements on the LAr purity in the T600 and considering the possible need to increase the sensitive volume, the ICARUS collaboration is studying the possibility to bring the T600 maximum drift from the present 1.5 m to 3 m, increasing the number of the field shaping rings while leaving untouched the wire chambers and the cathode
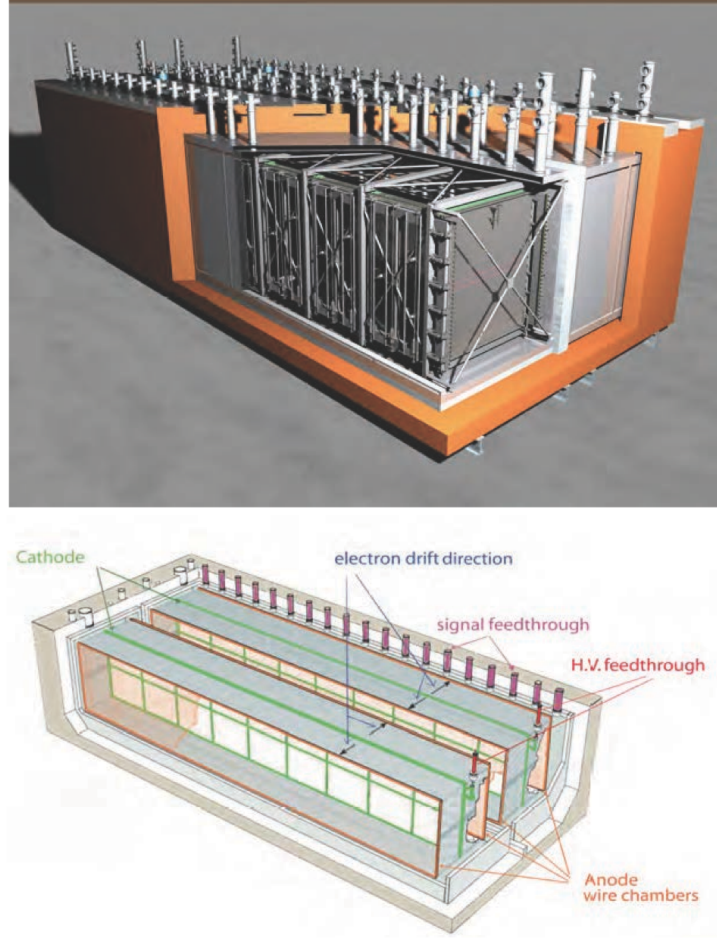
FIG. 16: *Top: ICARUS T600 detector schematics showing both modules and the common insulation surrounding the detector. The inner structures and feed-throughs are also shown. Bottom: A view of the detectors with the wire chambers and the high voltage system including race-tracks and cathodes.*

plane. Studies for doping of the LAr in order to enhance (linearize) energy response will also be part of the ICARUS continuing R&D program.

Finally, the option of implementing a 1 T magnetic field in the LAr sensitive volume by means of a pair of superconducting coils, will also be studied for future exploitation.

The above program will be carried out in the context of a joint effort of the ICARUS Collaboration and CERN. Installation and operation at Fermilab foresees a direct and significant involvement of Fermilab qualified personnel. All of the above mentioned activities will also bring considerable value as R&D for a future long-baseline neutrino facility based on LAr.

After overhauling the T600 components will be transported to Fermilab. They will arrive pre-assembled and tested to the maximum possible level, to minimize on-site assembly and

qualification operations. Discussions for safety acceptance and the relative standards with the Fermilab responsible people have already started. The cryogenics system will be described in Section IV D.

D. Cryostats and Cryogenics

The SBN program provides a first opportunity for the CERN and Fermilab engineering groups to collaborate on the design of LAr TPC infrastructure. Once established, this collaboration could have a significant impact on designs for other short and mid-term projects leading to a long-baseline neutrino facility. While most of the components of the T600 detector will be reused after overhaul at CERN, the LN2 delivery system is expected to be replaced and a completely new cryostat and cryogenics will need to be designed. The following describes the cryostat and cryogenic needs for the near and far detectors.

As described, the near detector will use a membrane tank technology to contain the base design of 180 tons of LAr (129 m^3) based on a scaled version of the LBNE 35 ton prototype. The cryostat will be housed in a dedicated building next to the existing SciBooNE hall where the cryogenic system components will be located. The cryostat will use either concrete or steel as its outer supporting structure; however, the foundation walls will not be used in the manner as described in the January PAC report [2]. Figure 17 shows a 3D model of the current design.

FIG. 17: *A 3D view of the LAr1-ND cryostat using membrane technology.*

The far detector will use a new inner cryostat to house the refurbished T600 detector. The cryostat will be enclosed in polyurethane foam insulation similar to that used for the membrane

cryostat of the near detector. The foam insulation will be contained in a new outer frame and LN2 shields will be used for heat interception. Figure 16 shows a 3D model of the proposed design.

The near and far detector cryogenic designs are being developed with a focus on commonalities which can be used across both experiments and also as a stepping stone for LBNF collaborative efforts. These systems will be modular in design and constructed on skids that can be tested separately prior to delivery to Fermilab for installation. Figure 18 outlines the basic LN2 supply system which is proposed by CERN and agreed as an appropriate solution for both detectors. Each experiment will rely on LN2 tankers for regular deliveries to local dewar storage. Storage dewars will be sized to provide several days of cooling capacity in the event of a delivery interruption. Note that for the far detector, the original Stirling machines used at Gran Sasso will not be used in the LN2 cycle. The lower estimated heat leak of the newly designed vessels allows for use of an open loop system typical of other LAr TPC vessels operated at Fermilab (LAPD, LAr35, and MicroBooNE).

Figure 19 shows a schematic diagram of the proposed LAr1-ND liquid argon system. It is based on experience in the design of the LNBE 35t prototype and the MicroBooNE detector systems. Figure 20 shows a schematic diagram of the T600 argon system including the existing LN2 refrigerators. These refrigerators would be replaced by a system like that shown in Figure 18 (bottom).

E. Civil Construction

The new building at 100 m incorporates conventional facilities to provide the spatial and infrastructure requirements required to assemble, install, and operate the physics components that comprise the near detector. Figure 21 shows a concept for the near detector building in cross section. In general, the construction will consist of a 1,300 square foot, below-grade enclosure centered on the existing Booster Neutrino Beam that will house the LAr TPC and related electronics while the 2,300 square foot above-grade portion will provide a means for staging and installing the detector components as well as personnel access. The below grade construction will be designed to bear the load up of up to 3 m of concrete shielding placed over the pit inside the building. This shielding can be added after detector installation if needed to reduce cosmogenic backgrounds. The site work will include utility extensions from MI-12, cryogenic storage tanks, gravel staging areas and vehicle access to the near detector building.

Similarly, the new far detector building incorporates the conventional facilities to provide the spatial and infrastructure requirements required to assemble, install, and operate the physics components that comprise the T600 far detector. In general, the construction will consist of a 8,500 square foot below-grade enclosure housing the relocated T600 detector as well as related electronics while the 7,500 square foot above-grade portion will provide a means for staging and installing the detector components as well as personnel access. The site work will include utility extensions from existing utility corridors, storage tanks, gravel staging areas, and vehicle
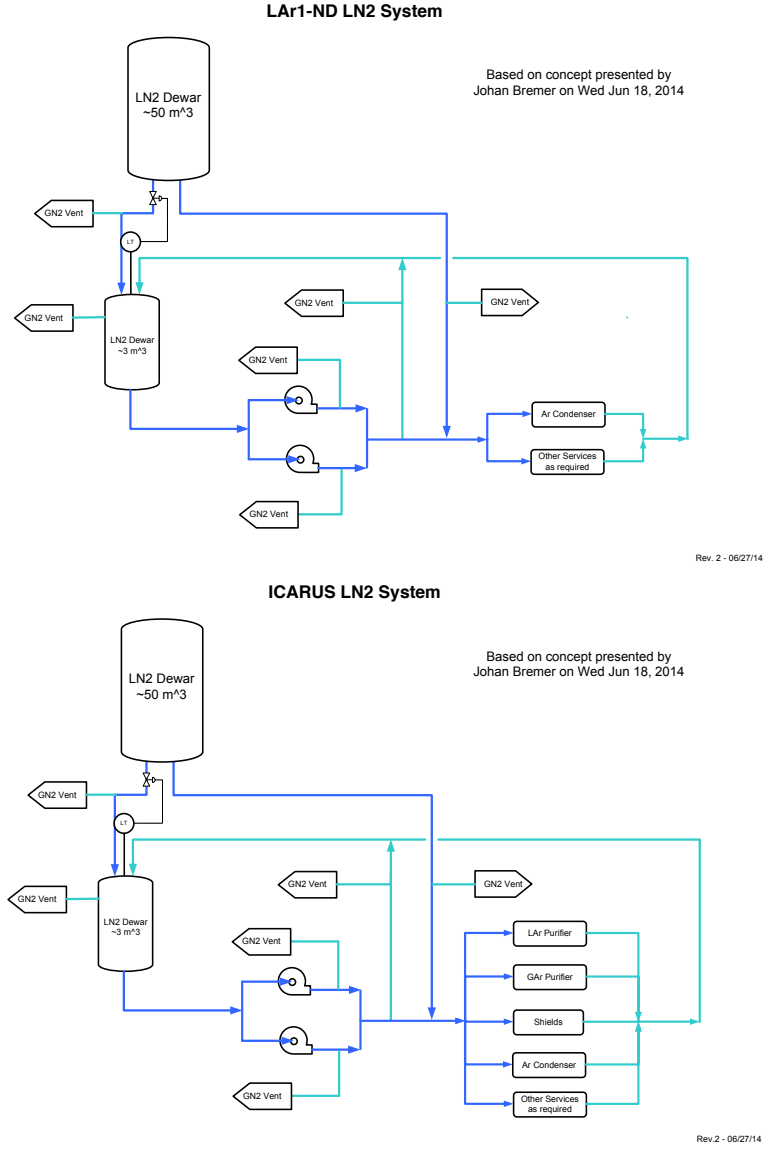
FIG. 18: *Schematic diagram for the proposed LN2 systems for LAr1-ND (top) and T600 (bottom).*

access to the far detector building. The building will be designed to accommodate up to 9.84 feet (3 meters) of earth equivalent shielding over the below grade detector enclosure if this is found to be needed to reduce cosmogenic backgrounds.

The primary installation challenge for the T600 is that the detector will be delivered to Fermilab as two cryostats with the TPCs already installed each weighing approximately 50 ton with dimensions of approximately 4 m wide × 4.2 m high × 20 m long. These cryostats need to be lowered into the new insulation system inside the building. Figure 22 shows one design concept for the far detector building. Several concepts are being considered to address the
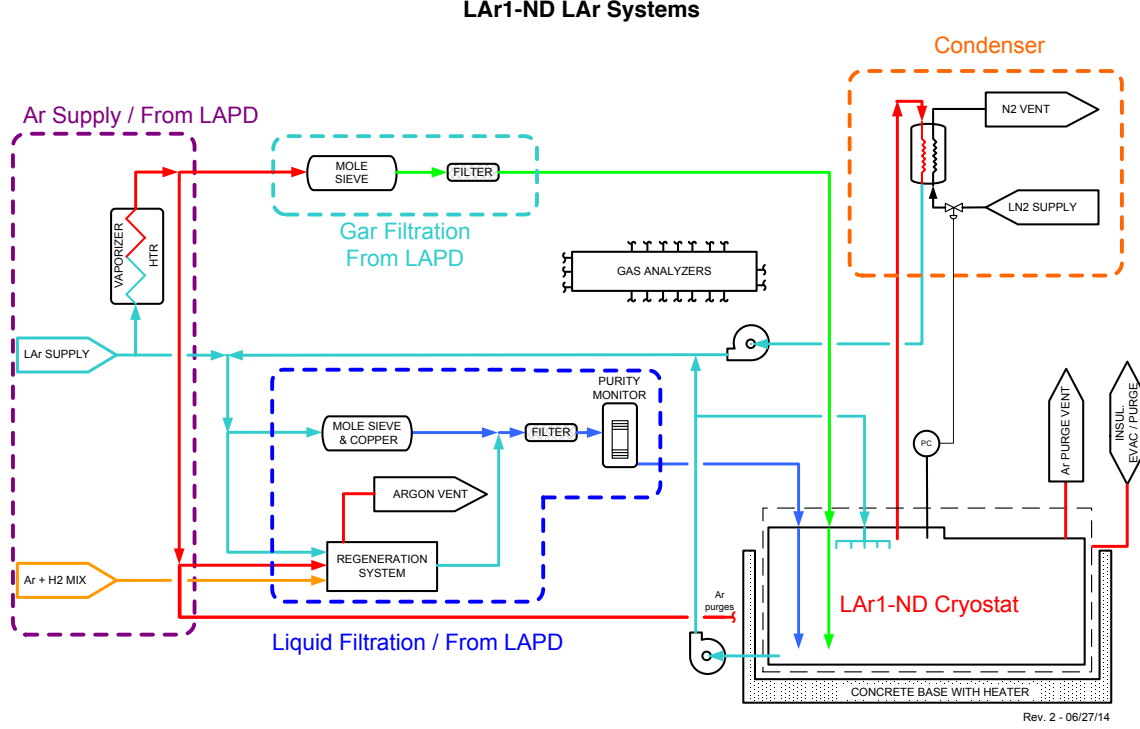
LAr1-ND LAr Systems

FIG. 19: *Schematic diagram for the proposed LAr1-ND liquid argon systems.*

installation and operational constraints of the T600 detector while staying within the GPP cost constraints.

F.   Re-Optimization of BNB Target and Horn

The Booster Neutrino Beamline (BNB) was originally optimized for the MiniBooNE detector. One of the considerations when designing the beamline was to increase the flux at 500 MeV, while reducing the flux at higher energies. The high energy neutrinos produce NC π^0s which in the MiniBooNE detector present significant background for the ν_e appearance measurement. The LAr TPC technology provides much better background rejection, and maximizing flux at all energies should be more beneficial. Several options are being considered which could lead to significantly increased neutrino flux and better optimized neutrino beam for the future SBN program at Fermilab. These are discussed below.

The power of horn focusing varies as a function of momentum and angle of a pion emitted from the target. The shape of the inner conductor in the presently used horn was optimized using the hadron production data available at the time. Since the horn was originally designed, precise measurements of pion production in the beryllium target have been made by the HARP experiment [24] and the kinematic distributions are now much better known. This allows for
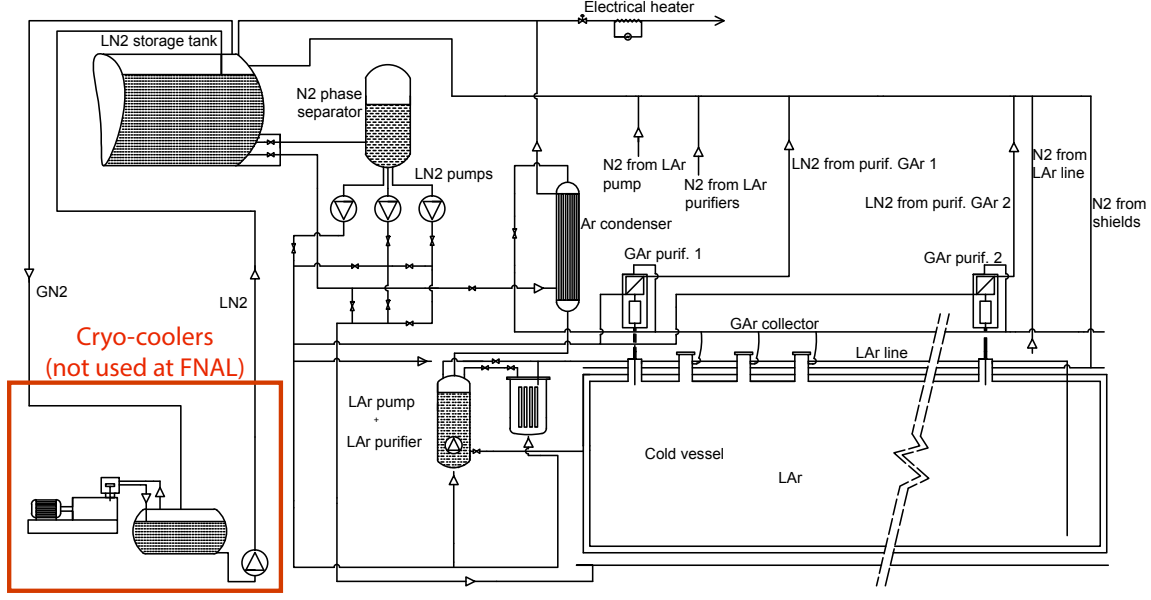
FIG. 20: *Schematic diagram of T600 cryogenic system. The section in the lower left would be replaced by the new liquid nitrogen delivery system show in Figure 18.*

more precise optimization of the inner conductor. Furthermore, the optimization goal for LAr TPC experiments, as discussed above, is somewhat different and a horn efficiently focusing higher momentum pions as well as lower momentum pions would be more optimal. So far, such re-optimizations of the inner conductor shape have yielded flux improvements on the order of only 8% but studies are continuing. Lastly, with gained experience building and running the BNB horn it is also worth revisiting the thickness of the horn conductor. At present, approximately 20% of the flux is lost due to pion interactions in the horn material. Using thinner conductors would reduce the losses.

The original design of the BNB beamline was based on the BNL beamline with 2 horns. Earlier studies showed that a second horn could increase neutrino fluxes by about a factor of two. The bulk of the increase would be in the higher energy part of the spectrum, with a 50% increase expected in the peak region. For the MiniBooNE detector this did not improve the signal to background ratio, however this may not be the case for LAr TPC detectors, and adding a second horn is a viable option. Although the BNB target hall was designed for a one horn system, it is possible to replace 3 long quadrupole magnets in the pre-target area with a much shorter set of magnets possibly freeing enough space to fit two horns into the existing enclosure. Reusing the same enclosure avoids significant costs of reconfiguring the target hall building.

Finally, the choice of target material is being studied. The target material provides a very useful handle in optimizing the neutrino spectrum. The BNB uses a 71.1 cm long beryllium target. The target material was chosen for practical reasons; to allow efficient air-cooling and
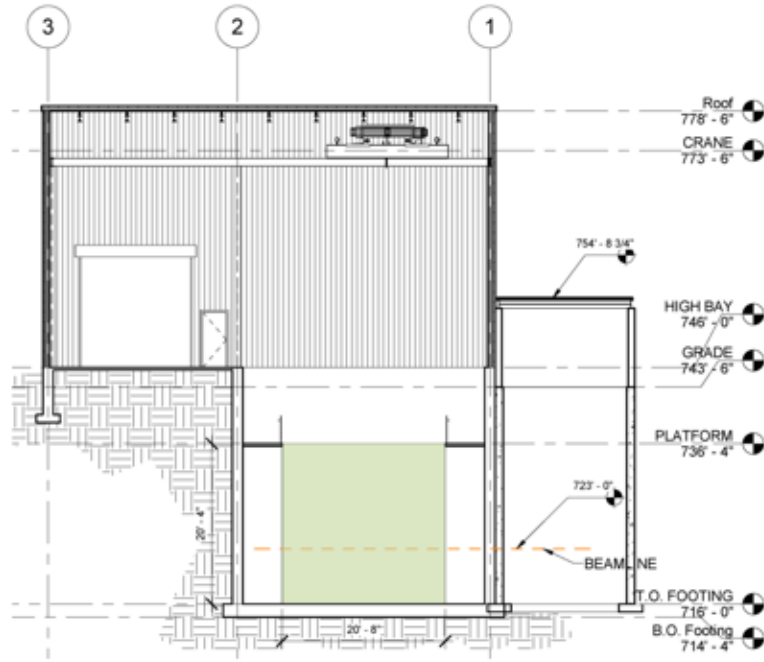
FIG. 21: *Cross-sectional view of a design concept for the building that will house the near detector (highlighted in green) below-grade. The design includes a surface building. The existing SciBooNE enclosure to the right will be used for the cryogenic system. The beam enters from the right in this view.*

produce less residual radioactivity. Over the last decade, a lot of experience handling heavier targets has been developed at Fermilab. With heavier materials it is possible to build shorter targets while maintaining the same interaction length. Since a horn focal length depends on particle momentum, relatively higher momentum particles are focused from the upstream end of the target compared to the downstream end. This results in a broader spectrum for long targets, and more peaked spectrum for shorter targets. Preliminary studies of the yields were done comparing beryllium, carbon, inconel and tungsten targets indicating that inconel provides the most flux in the peak.

These options, possibly providing more neutrino flux per proton and a better optimized spectrum which maximizes sensitivity in the region of interest, are presently being investigated further.
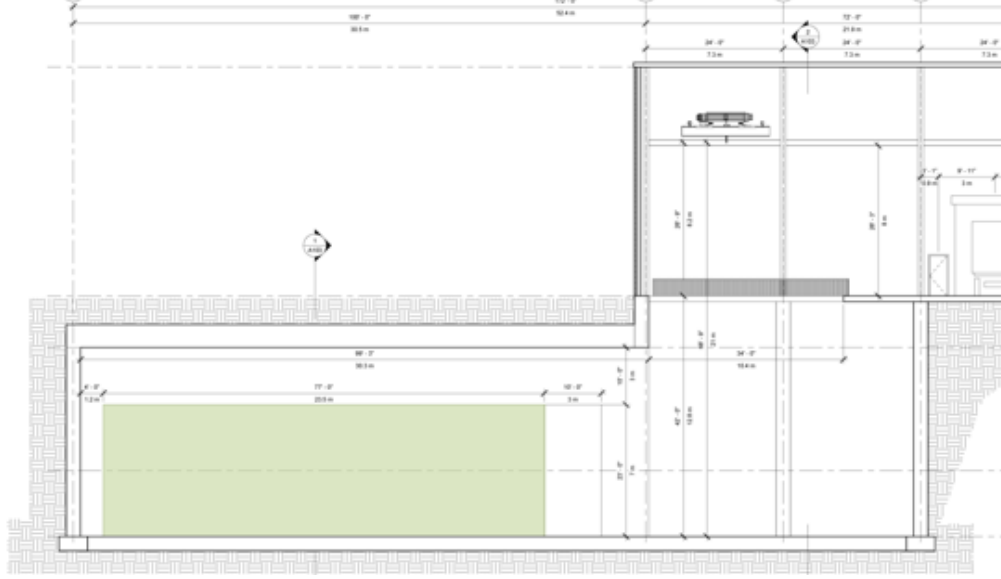
FIG. 22: *Cross-sectional view of a design concept for the far detector building. The T600 cryostat (highlighted in green) will be housed in the below-grade section portion. Equipment can be lowered into the below-grade area from the surface building using a crane. The beam enters from the left in this view.*

V. FUNDING, SCHEDULE AND ORGANIZATION

A. Schedule and Milestones

Initial data-taking with all three detectors operational is foreseen in spring 2018. By this time, the MicroBooNE detector will already have been operational with beam for several years. All steps to prepare the near and far detectors must be accomplished by this time, from the submission of the initial design report to startup of the civil engineering work, construction of cryostats and cryogenics, preparation of the T600 ICARUS detector, construction of the near detector, and overall detector preparation and commissioning. The proposed schedule is very tight, but with a good level of coordination, it is judged to be feasible.

At this stage of the program, it is better to define a set of milestones which define the necessary steps (Table IV). A detailed schedule for each activity will follow and will be centrally integrated. This report describes some intial steps toward the first milestone on the table. We anticipate that the conceptual design will be presented to the PAC as a proposal and to a technical, cost and schedule review called by the Fermilab Director.

Milestone	Date
Submission of a detailed SBN proposal for peer review	Oct 2014
Final CE requirements ready final building design	Nov 2014
Near detector cryostat engineering study contracted	Nov 2014
T600 at CERN, refurbishing starting	Dec 2014
Cryogenic plants proposal submitted for peer review	Mar 2015
LAr1-ND technical proposal submitted for peer review	Mar 2015
Ground breaking for far detector building	May 2015
Cryogenics procurement plans released and active	Sep 2015
Ground breaking for near detector building	Oct 2015
LAr1-ND cryostat procurement contract issued	Dec 2015
Buildings ready, utilities installation start	Oct 2016
Start cryostat assembly for near detector at Fermilab	Oct 2016
T600 ready at CERN for transport	Nov 2016
T600 detector arrives at Fermilab	Mar 2017
Start LAr1-ND detector installation	Apr 2017
Start cryogenic plant commissioning	Aug 2017
LAr1-ND and T600 installed	Sep 2017
Start detectors cooling and commissioning	Nov 2017
Start data taking with beam	Apr 2018

TABLE IV: *Milestones for construction, installation and initial commissioning of the Short Baseline Neutrino Program*

B. Funding

The funding of the overall program is foreseen to have several sources of funding from the U.S. and Europe. As the host laboratory, Fermilab will be responsible for the design, construction and outfitting of the buildings for the near and far detectors. It is expected that this construction will be funded as DOE General Plant Projects (GPPs). The maximum cost of a GPP ($10M) is a significant constraint for the design of the far detector building. A funding limit of $3M is placed on the near detector building based on total funding available at Fermilab for civil construction during this period. The design and construction starts of the far and near detector facilities are staged to match expected funding profiles yet provide beneficial occupancy in time for detector installation.

Costs for cryostats and cryogenics infrastructure will be shared between Fermilab, CERN, and INFN. CERN and INFN will act with in-kind contributions of engineering and procurements which can be done in Europe (e.g. near detector cryostat material, LAr cryogenic plants components, and existing T600 infrastructure components). The overhauling of the T600 at

CERN is financed by the WA104 collaboration through an MOU with CERN. Transport of components to Fermilab will be financed in the same way.

The construction of the new near detector (e.g. TPC, light detection) is expected to be financed by several funding agencies including the DOE, NSF, UK-STFC, and Switzerland. The exact sharing of responsibility will be defined in a dedicated MOU or MOUs, which will be monitored by Fermilab.

All operation costs will be defined in due time in a dedicated MOU, shared by all partners.

C. Organization

The SBN program, which is based on strong relations between different international partners and hosted by Fermilab, will need to operate through a clear set of well-structured responsibilities. Responsibility for the core of the activities will be born by the three international collaborations (LAr1-ND, MicroBooNE, and ICARUS), which will operate jointly while keeping their internal metabolism and management structure at least through the construction and installation phase. We expect all relations between the collaborations and Fermilab will be defined in dedicated MOUs.

Successful completion of the construction and installation of the detectors in a timely fashion will require careful coordination including technical, cost, and schedule reviews. We suggest that peer reviewing of progress be organized by Fermilab, in the form of Director's Reviews.

We further suggest that the Fermilab Directorate organize a proper Review Resource Board structure where the various funding agencies will follow the project and will agree on the level of resources to be allocated to the project year by year. The Fermilab Director (or designee) would chair and convene this board twice per year.

The complexity of the program, interdependence of the various detectors, and relation with the host laboratory will require coordination by an effective steering group. The composition of this steering group will need to be negotiated. However, a logical structure would be similar to the existing SBN task force with one representative per detector plus a few coordinators appointed by Fermilab management in consultation with CERN and INFN.

VI. ACKNOWLEDGMENTS

Within the working groups, members of all three collaborations, LAr1-ND, MicroBooNE and ICARUS have made major contributions to this work. In addition, members of the CERN and Fermilab staffs have provided valuable input.

––––––––––––––––

[1] M. Antonello *et al.*, "ICARUS at FNAL", proposal P-1052 submitted to the Fermilab PAC in January 2014,
`http://www.fnal.gov/directorate/program_planning/Jan2014PACPublic/ICARUS.pdf`.

[2] C. Adams *et al.*, "LAr1-ND: Testing Neutrino Anomalies with Multiple LAr TPC Detectors at Fermilab", proposal P-1053 submitted to the Fermilab PAC in January 2014,
`http://www.fnal.gov/directorate/program_planning/Jan2014PACPublic/LAr1ND_Proposal.pdf`.

[3] K. N. Abazajian et al., "Light Sterile Neutrinos: A White Paper", hep-ph/1204.5379 (2012).

[4] J. Kopp et al., "Sterile Neutrino Oscillations: The Global Picture". hep-ph/1303.3011 (2013).

[5] A. Aguilar-Arevalo *et al.* [LSND Collaboration], "Evidence for neutrino oscillations from the observation of anti-neutrino(electron) appearance in a anti-neutrino(muon) beam," Phys. Rev. D **64**, 112007 (2001) [hep-ex/0104049].

[6] MiniBooNE Collaboration, A. A. Aguilar-Arevalo et al., "A Search for Electron Neutrino Appearance at the $\Delta m^2 \sim 1$ eV^2 Scale," Phys. Rev. Lett. **98** (2007) 231801.

[7] MiniBooNE Collaboration, A. A. Aguilar-Arevalo et al., "Unexplained Excess of Electron-Like Events From a 1 GeV Neutrino Beam." Phys. Rev. Lett. **102** (2009) 101802.

[8] MiniBooNE Collaboration, A. A. Aguilar-Arevalo et al., "Improved Search for $\bar{\nu}_\mu \to \bar{\nu}_e$ Oscillations in the MiniBooNE Experiment", Phys. Rev. Lett. 110 (2013) 161801.

[9] MiniBooNE Collaboration, A. A. Aguilar-Arevalo et al., "A Search for Electron Anti-Neutrino Appearance at the $\Delta m^2 \sim 1 eV^2$ Scale", Phys. Rev. Lett. 103 (2009) 111801.

[10] T. A. Mueller et al., "Improved Predictions of Reactor Antineutrino Spectra", Phys. Rev. **C83** (2011) 054615.

[11] P. Huber, "On the Determination of Antineutrino Spectra From Nuclear Reactors", Phys. Rev. **C84** (2011) 024617.

[12] G. Mention et al., "The Reactor Antineutrino Anomaly", Phys. Rev. **D83** (2011) 073006.

[13] W. Hampel *et al.* [GALLEX Collaboration], "Final results of the Cr-51 neutrino source experiments in GALLEX," Phys. Lett. B **420**, 114 (1998). , J. N. Abdurashitov *et al.* [SAGE Collaboration], "Measurement of the response of the Russian-American gallium experiment to neutrinos from a Cr-51 source," Phys. Rev. C **59**, 2246 (1999) [hep-ph/9803418].

[14] V. Kudryavtsev, Private communication; D. Barker et al. "Muon-induced background for beam neutrinos at the surface", LBNE-doc-6232, August 2012; D. Barker et al. "Cosmic-ray background for beam neutrinos at the surface",LBNE-doc-6476, October 2012; LBNE Collaboration. "Scientific Opportunities with the Long-Baseline Neutrino Experiment", FERMILAB-CONF-13-300.

[15] C. Hagmann et al. "Cosmic-ray shower generator (CRY) for Monte Carlo transport codes". Nuclear Science Symposium Conference Record, 2007. NSS '07. IEEE (Volume:2).

[16] A. Ferrari, P.R. Sala, A. Fasso, and J. Ranft, "FLUKA: a multi-particle transport code". CERN-2005-10 (2005), INFNTC_0511, SLAC-R-773.

[17] A. Ereditato *et al.*, arXiv:1406.6400 [physics.ins-det].

[18] MicroBooNE project, "The MicroBooNE Technical Design Report", CD3b review, February 2012, `http://www-microboone.fnal.gov/publications/TDRCD3.pdf`

[19] T. Briese *et al.*, JINST **8**, T07005 (2013).

[20] C. Rubbia *et al.*, JINST **6** P07011 (2011).

[21] S. Amerio *et al.*, Nucl. Instr. and Meth. **A527** 329-410 (2004).

[22] M. Antonello *et al.*, EPJ **C73**, 2345 (2013).

[23] M. Antonello *et al.*, EPJ **C73** 2599 (2013).

[24] HARP Collaboration, M.G. Catanesi et al., "Measurement of the Production Cross-Section of Positive Pions in the Collision of 8.9 GeV/c Protons on Beryllium", Eur. Phys. J. **C52** (2007) 29-53, hep-ex/0702024.